

## Collective Nuclear Structure in the Even-Even Samarium Isotopes\*

G. G. SEAMAN,<sup>††</sup> J. S. GREENBERG, AND D. A. BROMLEY  
*Yale University, New Haven, Connecticut*

AND

F. K. MCGOWAN  
*Oak Ridge National Laboratory, Oak Ridge, Tennessee*  
 (Received 7 March 1966)

The level structure and transition matrix elements between collective states in the even-even isotopes of samarium ( $A=148-154$ ) have been investigated using Coulomb excitation induced by  $O^{16}$  ions. Both total and differential cross sections were measured for the de-excitation gamma radiation and for gamma radiation in coincidence with the inelastically scattered oxygen ions. Internal-conversion data also supplemented some phases of these studies. The existing information on these nuclei has been extended to include higher spin states and previously unmeasured transition moments for both even- and odd-parity states. The predictions of the available phenomenological collective models have been compared with this information and it has been found that although the latter models can account for some of the general features of the observed excitation spectra and transition matrix elements, they are deficient in explaining the details. In  $Sm^{152}$ , where specific attention was devoted to the levels associated with the beta and gamma vibrations, the results indicate that for nuclei near the edges of the deformed region the axially symmetric model, with a first-order perturbation treatment of the rotational-vibrational interaction, is not adequate to explain the structure of low-lying states, and that this mechanism can account for only 9% of the observed coefficient of the second-order term in the expansion of the excitation energy in an angular-momentum power series. The more exact account of centrifugal stretching, developed by Davydov and Chaban, presently produces the best over-all fit, but a number of discrepancies with the data still remain and are discussed.

### I. INTRODUCTION

THE description of the static and dynamic properties of the low-lying even-parity states in a large class of nuclei in terms of phenomenological rotator and vibrator models has met with considerable qualitative and some quantitative success. The usefulness of this approach has been substantiated by the continual discovery of rotational bands in a large number of nuclei throughout the periodic table. In recent years considerable progress has also been made toward a fundamental understanding of the microscopic aspects of collective behavior; it has become possible to evaluate some of the collective parameters, introduced phenomenologically in the models, with fair accuracy.<sup>1-7</sup>

Extensive comparisons have been made of experiment with the theory of rotational excitation spectra developed, both for axially symmetric and for nonaxial deformed nuclei, in the adiabatic approximation in

which the rotation of the nucleus takes place without coupling to its intrinsic states or collective vibrations. Although a large body of data satisfies the characteristic main features of such a rigid-rotator model with reasonable precision, the more extensive and precise measurements that have been made recently on high-spin members of rotational bands, and especially on electromagnetic transition probabilities between collective states, show that detailed agreement is lacking between these simple strong-coupling rotational models and experiments. Attempts have been made to account for these deviations by relaxing the artificial adiabatic requirement and including specifically the interaction between rotations and vibrations. These attempts at a phenomenological description have developed along two principle approaches. The two approaches differ as to the assumptions made for the static nuclear equilibrium shape, and the treatment of the centrifugal stretching effects. Both are described briefly below and more fully in Secs. V and VI of this paper, where they are applied to the specific case of  $Sm^{152}$ .

In one description by Bohr and Mottelson,<sup>8,9</sup> the properties of the lowest lying even parity levels, resulting from rotation and vibrations of a quadrupole deformed nuclear surface, are derived on the simplifying assumption that the equilibrium shape of the deformed nucleus retains axial symmetry and that the projection of the total angular momentum along the symmetry axis  $K$ , to a good approximation is a constant of the motion. In the adiabatic limit, the predicted energy

\* Supported by the U. S. Atomic Energy Commission.

<sup>†</sup> Present address: Los Alamos Scientific Laboratory, Los Alamos, New Mexico.

<sup>††</sup> Submitted in partial fulfillment of the requirements for degree of Doctor of Philosophy to the Graduate School of Yale University.

<sup>1</sup> S. G. Nilsson and D. Prior, *Kgl. Danske Videnskab. Selskab, Mat. Fys. Medd.* **32**, No. 16 (1961).

<sup>2</sup> J. J. Griffin and M. Rich, *Phys. Rev.* **118**, 850 (1960).

<sup>3</sup> S. T. Beliaev, *Kgl. Danske Videnskab. Selskab, Mat. Fys. Medd.* **31**, No. 11 (1959).

<sup>4</sup> D. J. Thouless and J. G. Valatin, *Phys. Rev. Letters* **5**, 509 (1960).

<sup>5</sup> G. E. Brown, *Lectures on the Many Body Problem from the First Bergen International School of Physics, 1961*, edited by C. Fronsdal (W. A. Benjamin, Inc., New York, 1962), p. 164.

<sup>6</sup> V. Radojevic, A. Sobczewski, and Z. Szymanski, *Nucl. Phys.* **38**, 607 (1962).

<sup>7</sup> P. C. Hemmer, *Nucl. Phys.* **32**, 128 (1962).

<sup>8</sup> A. Bohr, *Kgl. Danske Videnskab. Selskab, Mat. Fys. Medd.* **26**, No. 14 (1952).

<sup>9</sup> A. Bohr and B. R. Mottelson, *Kgl. Danske Videnskab. Selskab, Mat. Fys. Medd.* **27**, No. 16 (1953).

spectrum is that of a pure rotator, based on the ground-state, vibrational, and other intrinsic excitations, and the calculated transition intensities to or from the member states of a rotational band are proportional only to the squares of vector-addition coefficients. Deviations from the adiabatic condition, arising from effects such as small dynamic departures from axial symmetry due to gamma-type vibrations, and centrifugal stretching with vibrations of the beta type which preserve axial symmetry, are treated in perturbation theory. The zeroth-order wave functions in this treatment are those of a rigid axially symmetric rotor. These perturbations admix bands of  $\Delta K=2, 0$ , respectively, in first order, and result in energy spectra that deviate from the simple rotational rule; in a more spectacular way they modify the interband electromagnetic transition probabilities.<sup>10</sup> These latter reflect a coherent sum of the individual transition amplitudes between all components of the admixed initial- and final-state wave functions. Since transition matrix elements between components of the wave functions based on the same rotational band are proportional to the large static quadrupole moment, the parts of the total matrix element involving even small admixed wave-function components may be correspondingly enhanced to play a significant role in the interband transitions. In effect, the intraband collective enhancement acts to amplify the contribution of weak wave-function components involved in the interband transitions. Thus, study of these interband transition probabilities between admixed bands provides a sensitive measure of band-mixing effects.

In considering the effect of the perturbations on the ground-state band of even-even nuclei where  $K=0$ , the rotational energy of the latter may be expanded in a power series in the total angular momentum, with the leading term representing the adiabatic approximation, and the second and higher order terms originating successively from perturbations expressed in increasing powers of the angular momentum.

$$E_{\text{rot}} = AI(I+1) + BI^2(I+1)^2 + CI^3(I+1)^3 + DI^4(I+1)^4 + \dots \quad (1)$$

Such an expansion, of course, is only useful in comparisons with experiment if the series converges rapidly so that the number of terms, or free parameters, is kept small. When high-spin,  $K=0$ , rotational states have been established for nuclei where the excitation ratio  $E(4^+)/E(2^+) < 3.27$ , the convergence has been found to be slow; this perturbation expansion thus may not be appropriate in these cases. This lack of convergence may result from strong coupling between bands, in which case a more exact treatment of the perturbing interaction is required, as will be discussed below.

<sup>10</sup> O. B. Nielsen, in *Proceedings of the Rutherford Jubilee International Conference*, edited by J. B. Birks (Heywood and Company, London, 1962), p. 137; J. Borggreen, O. B. Nielsen, and H. Nordby, *Nucl. Phys.* **29**, 515 (1962).

If, however, the interaction between bands is assumed to be weak enough so that the correction to the rotational energy spectrum is predominantly represented by the second term in the perturbation expansion, the mixing of vibrational band members with the ground-state band members may be adequately described by considering only first-order mixing of the wave functions. Of particular interest in a  $K=0$  nucleus is the extent to which the ground-state rotational band and the beta ( $K=0$ ) and gamma ( $K=2$ ) vibrational bands are admixed due to the perturbation effects already mentioned, arising from centrifugal stretching and dynamic deviations from axial symmetry. In the Bohr Hamiltonian<sup>8,9</sup> the operators that can be identified with the coupling of the  $K=0$  ground-state band to the beta band ( $\Delta K=0$ ) and gamma band ( $\Delta K=2$ ) are, respectively,  $(I_1^2 + I_2^2)$  and  $(I_1^2 - I_2^2)$ , where the notation is standard and the angular-momentum operators refer to the nuclear-body-fixed axis. The matrix element for the latter operator obviously vanishes for a static spheroidal model. Since the first-order mixing coefficients for the two bands, involving matrix elements of the above operators, appear in the transition probabilities between bands, they can be deduced from the experimentally measured interband transition rates and branching ratios. More than one experimental branching ratio is desirable from several members of the excited band to levels in the ground-state band to verify the angular-momentum dependence of the perturbing interaction given above for the beta and gamma bands, and to establish internal consistency. The mixing coefficients also enter quadratically in the expression for the energy in the usual manner through second-order perturbation theory. Therefore, the corresponding shift in the energy levels from the adiabatic approximation may then be calculated and compared with the coefficients  $B$ , found from fitting Eq. (1)<sup>10</sup> to the experimentally determined level spectrum. This analysis can obviously be extended in principle to higher order in perturbation theory, if such a perturbation expansion is valid.

It should be noted that except for the assumption of strong coupling, the analysis procedure outlined above can be carried out in a model-independent way without any assumptions as to the form of the moments of inertia. However, in the lowest order treatment discussed above, the variation of the moment of inertia with the angular momentum is excluded.

Initial investigation of these effects assumed that mixing of the ground-state and gamma vibrational bands was the dominant perturbation. Nielsen and co-workers<sup>10</sup> have examined the experimental evidence bearing on such gamma-band mixing in a number of nuclei in which levels in the gamma band have been identified systematically. Applying the analysis outlined above, they have found that this mixing could account for only 5–10% of the observed energy depression of the ground-state band levels.

The extent of the beta-band mixing in such an analysis scheme has not been established with a reliability equal to the gamma-band-mixing contribution because of the scarcity of experimental information on the beta band levels and their de-excitation. The empirical correlation between the depression in energy of the first excited  $0^+$  levels, where these have been identified, and the magnitude of the coefficient  $B$  in Eq. (1) would suggest that the presence of low-lying beta vibrational excitations is closely associated with the deviations from a  $I(I+1)$  energy spacing in the ground-state rotational band. Theoretical calculations of the coefficient  $B$  within the framework of a pairing model,<sup>6,11</sup> and experimental information from earlier experiments<sup>12,13</sup> also indicated that the effect of mixing with the beta band could exceed that of mixing with the gamma band. Some of the measurements described below were undertaken to explore in detail the rotational-vibrational interaction with the beta band, motivated by the above suggestions that contributions to  $B$  from beta-band mixing may be large.

The second approach, noted above, to the description of collective rotational spectra assumes that, in general, the equilibrium shape can be axially asymmetric ( $\gamma \neq 0$ ). The case in which the three nuclear moments of inertia are related by the hydrodynamic approximation and the adiabatic limit is assumed has been examined by Davydov and Fillipov<sup>14</sup> and by Davydov and Rostovsky.<sup>15</sup> This asymmetric-rotor model has had qualitative success in reproducing the energy-level spectra and electromagnetic transition probabilities in a significant number of nuclei. Mallman and Kerman<sup>16</sup> have incorporated a rotational-vibrational interaction in this model in a perturbation approach similar to the one discussed above for the axially symmetric case, and have been able to improve and extend the agreement with experiment. Generally, the agreement with experiment is better than that achieved with the first-order correction to the axially symmetric model. However, for transition nuclei, such as Sm<sup>152</sup>, Gd<sup>154</sup>, and some of the osmium isotopes, the agreement is poor. In addition, the values for  $\gamma$  calculated from observed transition probabilities do not agree with the values obtained from fits to the observed energy-level spectra.<sup>17</sup>

A more exact treatment of the beta vibrations, within

the framework of the hydrodynamic asymmetric-rotor model, has been developed by Davydov and Chaban.<sup>18</sup> The hydrodynamic form is taken for the moments of inertia.<sup>8</sup> Centrifugal stretching is included directly as a potential term with a quadratic dependence on  $\beta$  in the zeroth-order Hamiltonian. A harmonic approximation is used for the potential energy, and an allowance is made for the change of the equilibrium deformation with total angular momentum. This model assumes that the nucleus is rigid relative to gamma vibrations and includes the assumption that the centrifugal stretching will produce no large changes in the equilibrium value of  $\gamma$ . Vibrations of the  $\gamma$  type have been explicitly included in an extension of this model by Davydov.<sup>19</sup>

It may be noted that in the Davydov-Chaban treatment, the zeroth-order eigenvalues for the energy, which include the effects of centrifugal stretching, contain all powers of  $I(I+1)$ , and that perturbations such as may arise from anharmonic components in the potential energy merely add to the coefficients of the possible many terms in a series expansion in the angular momentum. Beringer<sup>20</sup> has further developed and extended the Davydov-Chaban approach to higher orders of perturbation theory for the energy eigenvalues, and demonstrated the rapid convergence of the higher correction terms to the Davydov-Chaban energies even for soft rotors. An examination of the zeroth-order energy eigenvalues in the above theory in a power-series expansion in  $I(I+1)$  shows that for nuclei in which the centrifugal distortion is expected to be appreciable, many higher order terms are required to produce an accurate representation for the energy eigenvalues which include the effects of centrifugal stretching. The latter result again indicates, as will the empirical evidence to be presented in detail in this paper and mentioned in the preceding discussion, that the rigid-rotor wave functions do not represent a convenient starting point for a perturbation analysis of rotational spectra in soft rotors.

A number of comparisons with experimental energy spectra have been made using the Davydov-Chaban calculations both for quite rigid and for soft rotors. As would be expected, for small values of the Davydov-Chaban "nonadiabaticity parameter,"  $\mu \leq 0.25$ , corresponding to quite rigid rotors, the results are essentially identical with those obtained by Kerman and Mallman using a perturbation approach. For such nuclei the axially symmetric model, with rotation-vibration interaction to first order, also yields the same agreement with experiment for the energy-level spectra. For  $\mu \leq 0.33$  the Davydov-Chaban calculations correlate well with the data available on energy spectra of ground-state and beta bands, although the predictions are not always within experimental error. Some qualitative suc-

<sup>11</sup> E. R. Marshalek, Phys. Rev. **139**, B770 (1965); E. R. Marshalek and J. B. Millazzo, Phys. Rev. Letters **16**, 190 (1966).

<sup>12</sup> J. S. Greenberg, G. G. Seaman, E. V. Bishop, and D. A. Bromley, Phys. Rev. Letters **11**, 211 (1963).

<sup>13</sup> F. S. Stephens, B. Elbek, and R. M. Diamond, in *Proceedings of the Third Conference on Reactions Between Complex Nuclei*, edited by Albert Ghiorso, R. M. Diamond, and H. E. Conzett (University of California Press, Berkeley, California, 1963).

<sup>14</sup> A. S. Davydov and G. F. Fillipov, Nucl. Phys. **8**, 239 (1958).

<sup>15</sup> A. S. Davydov and V. S. Rostovsky, Nucl. Phys. **12**, 58 (1959).

<sup>16</sup> C. A. Mallman and A. K. Kerman, Nucl. Phys. **16**, 105 (1960).

<sup>17</sup> G. T. Emery, W. R. Kane, M. McKeown, M. L. Perlman, and G. Scharff-Goldhaber, Phys. Rev. **129**, 2597 (1963).

<sup>18</sup> A. S. Davydov and A. A. Chaban, Nucl. Phys. **20**, 499 (1960).

<sup>19</sup> A. S. Davydov, Nucl. Phys. **24**, 682 (1961).

<sup>20</sup> E. R. Beringer (private communication, and to be published).

cess has also been achieved in applying the calculations for very soft rotors (where  $\mu > 0.35$ ) to nuclei near closed shells, although not without exceptions. Recently,<sup>21</sup> in an investigation of very high spin states in the ground-state band in a number of even-even nuclei, it was found that the dependence of the inertial parameters on the spin was reproduced in satisfactory fashion by these calculations, while the perturbation calculations leading to Eq. (1) based on an axially symmetric model apparently fail.

Such comparisons seem to suggest that the dynamic beta deformations may contribute significantly to the observed deviations from the simple rotational spectra, and because of the apparent magnitude of their influence, their interaction with the rotational motion is not amenable to perturbation calculations but requires a more exact treatment. The role of gamma vibrations, in the context of the Davydov-Chaban and Davydov models, has not been subject to any extensive experimental tests. As noted previously, however, there is considerable evidence to support the assumption that the gamma vibrations are not strongly coupled to the ground-state band, and therefore that perturbation methods are probably more applicable to the description of the interaction between gamma vibrations and pure rotations. Most of the experimental comparisons regarding the influence of the beta vibrations are concerned with their effect on the ground-state rotational spectra. In order to achieve a fuller understanding of this interaction it is essential to examine and confirm that the beta-band head, beta-band energy spacings, and the various interband transition probabilities as well as the ground-state band spectra form a consistent picture. Information relevant to such analysis is only now beginning to be accumulated.

It is evident from the above discussion that studies on nuclei in the transition region between highly deformed and spherical regions are particularly suited to examination of the interactions between vibration and rotation and to the evaluation of this interaction with changing nuclear rigidity. Examples of such transition nuclei are found near the edges of regions of strong stable deformation, e.g.,  $150 < A < 190$ . Here the low-lying level structure is characterized by the rapid rise of the first  $I=2$  state as the edge of the region is approached and by a decrease in the excitation energy ratio,  $E(0_{\beta}^+)/E(2_{gs}^+)$ , where the subscripts  $\beta$  and  $gs$  refer to the beta and ground-state bands, respectively. Some of the even osmium isotopes on the high-mass side of this region and the even Sm, Gd, and Nd isotopes on the low-mass side show this characteristic behavior. This paper is concerned with the low-lying collective levels in the even isotopes of Sm. These have been selected for study since the range from  $A=148$  to  $A=154$  appears to span the transition from vibrational to well-developed rotational structure.

<sup>21</sup> F. S. Stephens, N. L. Lark, and R. M. Diamond, Nucl. Phys. **63**, 82 (1965).

Coulomb excitation with  $O^{16}$  ions was used to populate the energy levels studied herein. Heavy projectiles were chosen for this work because of the correspondingly large cross sections for multiple excitation of the high-spin states in the ground-state and vibrational bands which are not normally accessible to conventional reaction and decay scheme studies. The energy levels usually associated with the beta band particularly fall into this category as indicated by the scarcity of relevant systematic information. The well-established characteristics of the Coulomb excitation reaction mechanism, involving only an electromagnetic interaction, have also been very helpful in identifying level characteristics and interpreting level schemes. Although these latter interpretations are sometimes model-dependent, reflecting a model-dependent description for some of the Coulomb excitation processes for heavy ions, the approximations used probably do not change the qualitative conclusions reached on this basis. Calculations of reduced transition matrix elements were performed using both the presently available multiple Coulomb excitation theories and, where the approximation was suitable, first- and second-order perturbation calculations. The former have undergone several modifications and extensions since the initial calculations using the sudden approximation were made available, and comparisons have been made between the various versions.

The work presented here was performed using both the Yale HILAC and the EN Van de Graaff accelerator at ORNL. The cw characteristics of the Van de Graaff were particularly important in coincidence experiments for which the relatively low-duty-cycle HILAC was not suitable. Some of the preliminary studies, carried out at the HILAC with  $O^{16}$  ions up to 64 MeV on previously unreported levels in  $Sm^{152}$  and  $Sm^{154}$  and on band-mixing calculations in  $Sm^{152}$ , have been reported elsewhere.<sup>12,22,23</sup> The present paper is concerned principally with the subsequent, more detailed, coincidence experiments that were performed with the EN Van de Graaff at an  $O^{16}$  ion bombarding energy of 49 MeV. Similar studies have also been completed on the even isotopes of Gd and Nd; these will be reported in detail in a forthcoming publication.

## II. EXPERIMENTAL PROCEDURE

The Coulomb excitation process was detected by observing gamma radiation from the de-excitation of the excited nuclear levels. In some cases the internal conversion electrons from selected transitions were also observed, principally to establish a  $0^+ \rightarrow 0^+$  decay sequence, where electron monopole conversion is the

<sup>22</sup> J. S. Greenberg, D. A. Bromley, and G. G. Seaman, *Proceedings of the Padua Symposium on Direct Interactions and Nuclear Reaction Mechanisms, Padua 1963*, edited by C. Villi and E. Clementel (Gordon and Breach, Science Publishers, Inc., New York, 1963).

<sup>23</sup> J. S. Greenberg *et al.*, in *Proceedings of the Third Conference on Reactions Between Complex Nuclei*, edited by Albert Ghorso, R. M. Diamond, and H. E. Conzett (University of California Press, Berkeley, California, 1963).

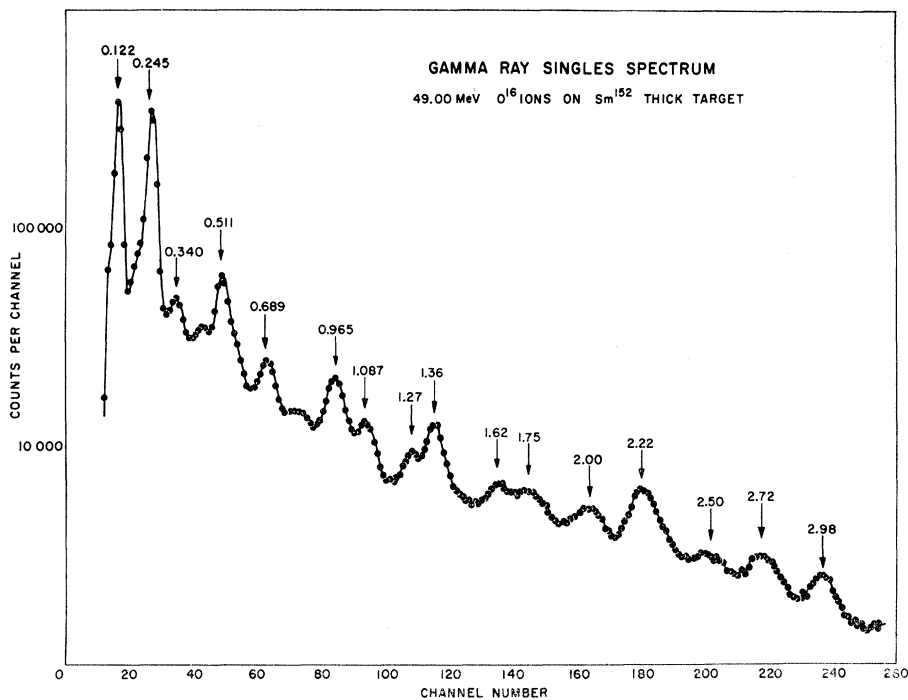


FIG. 1. Gamma-ray spectrum taken with a 3 in.  $\times$  3 in. NaI crystal for 49-MeV  $O^{16}$  ions on a thick target of  $Sm^{152}$ . All gamma rays indicated above  $\sim 1200$  keV in energy originate from reactions with low- $Z$  surface contaminants.

only mode of decay for transition energies below 1.02 MeV. Measurements were made of the direct gamma-ray spectra, of gamma rays in coincidence with the incident  $O^{16}$  ions scattered into the backward direction (hereafter called gamma-particle coincidences), and of gamma rays in coincidence with other gamma rays. Except for prominent transitions, the direct gamma-ray spectra were of limited usefulness for quantitative considerations principally because of background gamma radiation, arising from nuclear reactions with low- $Z$  target surface contaminants. The probable sources of such contaminants for the metallic targets used were oxidation of the target material itself and condensation of pump oil vapors.

Figure 1 is an example of a direct spectrum taken with 49-MeV  $O^{16}$  ions on  $Sm^{152}$ , and shows clearly some of these higher energy contaminant gamma rays. Those above 1.27 MeV were found to result from other than Coulomb excitation processes and occurred for every target. They are readily assigned to a number of well-known transitions in reactions of  $O^{16}$  ions with common low- $Z$  nuclei. An analysis of these possible contaminants showed that gamma rays with energies corresponding to 439, 686, 705, 824, 842, and approximately 1015 keV would be expected in the lower energy region of the spectra, where they can interfere with the identification of weakly populated levels from Coulomb excitation. Most of these radiations appeared in all the singles spectra taken, and were identified with the aid of the gamma-particle coincidence spectra, where they are absent for reasons discussed below. However, the intensities of the weak transitions arising from Coulomb

excitation could not be determined from the singles spectra alone.

Connected with this problem of low- $Z$  contaminants in the target was also the general requirement of pure oxide-free metallic targets. The Sm isotopes were available only in the form of an oxide compound from the supplier. When used in this form the total gamma-ray flux, arising largely from  $O^{16}$ - $O^{16}$  reactions, was prohibitive for any experiment in which a single gamma-ray counter was used, or for gamma-gamma coincidence measurements. Although gamma-particle experiments were feasible, the reduced data acquisition rate imposed by the high counting rate in the gamma-ray counter made such experiments almost impractical, especially with a low-duty-cycle machine such as the HILAC at Yale. A method was therefore developed at Yale<sup>22,23</sup> to produce pure metallic targets using a miniaturized version of a method of oxide reduction for rare-earth metals pioneered by Spedding and Daane.<sup>24</sup> All targets used were metallic.

The targets were prepared from separated isotopes. After the reduction of the  $Sm_2O_3$  to a pure metal they were evaporated in vacuum onto 0.00025-in. tantalum backings. Target thicknesses averaged approximately 25 mg/cm<sup>2</sup>, adequate for stopping 65-MeV  $O^{16}$  ions. The isotopic purity for  $Sm^{154}$  and  $Sm^{152}$  exceeded 99% and for  $Sm^{150}$  and  $Sm^{148}$  exceeded 96%. Techniques for preparing these targets will be published elsewhere.

For the more prominent gamma-ray transitions, the

<sup>24</sup> F. Spedding and A. Daane, *The Rare Earths* (John Wiley & Sons, Inc., New York, 1961).

direct spectra were used for determining the behavior (with incident-ion energy) of the relative excitation probabilities of various states. This information, together with the multiple-Coulomb-excitation theory, was utilized in assigning transitions. It is already evident from the complex spectrum shown in Fig. 1 that heavy-ion Coulomb excitation significantly populates a large number of excited states in contrast to the one or two states usually seen in similar measurements with light projectiles. As stated previously, this was one of the major reasons for choosing this technique. The gamma-gamma coincidence measurements provided information on the cascade relationships between the many radiations seen and were very important in translating these complex spectra into level schemes.

Experiments in which the gamma rays were detected in coincidence with back-scattered particles served several purposes. By suitably biasing the particle detectors (discussed explicitly below) so that nuclear reaction products were not counted, gamma rays from nuclear reactions could be eliminated from these spectra. Comparing spectra taken in this manner with those obtained directly or in gamma-gamma coincidence served to identify the contaminant gamma rays in the latter. A very significant reduction in the background was also achieved in the gamma-particle spectra. This together with the enhanced multiple excitation of higher lying levels, in these spectra reflecting the closer collision for backward-scattered ions, further extended the possibility of observing residual states with large angular momentum. With the aid of Coulomb excitation theory, spectroscopic information was obtained by comparing

the redistribution of the level population in the gamma-particle and direct spectra as a function of the incident-ion energy. Individual examples of the latter analysis are presented in the discussion below.

### III. APPARATUS

The target chamber used for the gamma-particle coincidence measurements is shown in Fig. 2. At the ORNL accelerator, direct gamma-ray spectra and gamma-gamma coincidence spectra were taken with a simplified chamber that insured more reliable beam integration. In the latter, the beam was collimated to a spot, 1 mm×6 mm in dimensions. Collimation for the experiments at the Yale HILAC was relaxed somewhat to yield a beam diameter on target of 0.25 in., reflecting the poorer optical properties of the beam. At both accelerators the beam of  $O^{16}$  ions was used in the  $6^+$  charge state. At the Yale HILAC the beam energy was varied from 16–64 MeV, while at the ORNL accelerator a fixed maximum available energy of 49 MeV was used.

The gamma-ray detectors were NaI(Tl) crystals; two crystal sizes were used,  $1\frac{1}{2}$  in.×2 in. and 3 in.×3 in. In the several experiments that were performed, they were positioned at  $55^\circ$ ,  $90^\circ$ , and at  $0^\circ$  to the incident-beam direction, and in the gamma-gamma coincidence measurements they were shielded from each other with a lead block to prevent cross-scattering. A number of the usual precautions were taken to stabilize drifts and to minimize counting-rate dependence for these counters.

Energy calibrations for the gamma-ray detectors were performed at the same counting rates as those used in the experiments, using standard gamma-ray sources.

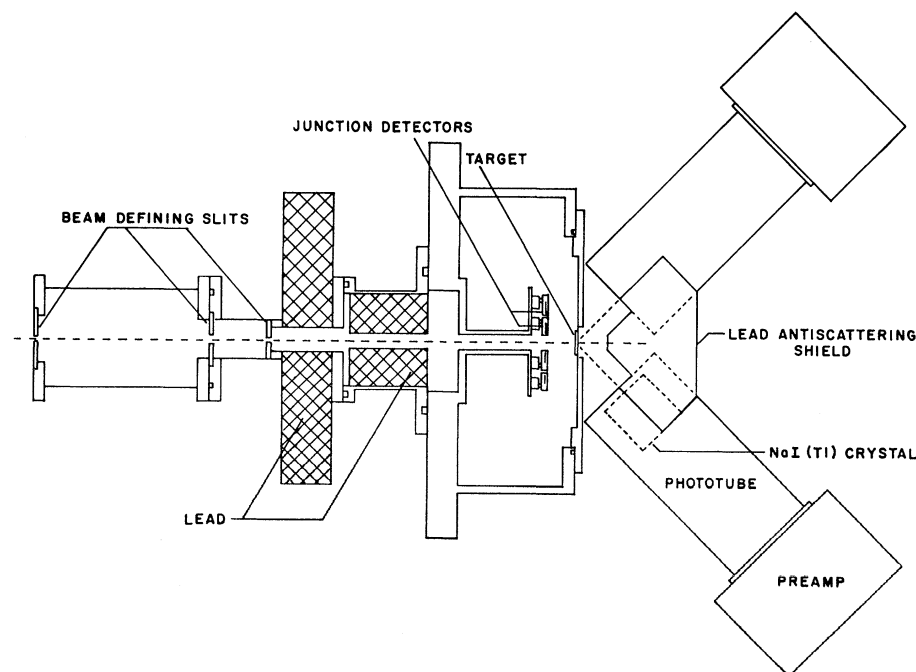


FIG. 2. Scattering chamber showing location of the silicon junction detectors. The locations of NaI detectors are shown only schematically; they are not necessarily the positions occupied by these detectors in the experiment.

These were supplemented by internal calibrations which employed the previously well-established transitions in the nuclei being studied. Crystal efficiencies were taken from calculations by Vegor, Marsden, and Heath<sup>25</sup> and from measurements by Heath.<sup>26</sup> The ratios of the photopeak to total efficiencies were checked experimentally and were found to agree with Heath's measurements. Monoenergetic gamma-ray sources, prepared on 0.00025-in. Mylar foil, were used to measure standard spectral shapes in counter geometries closely simulating those used in the experiments. A cross-calibration of the relative efficiencies between the geometries that were used in the actual experiments and the standard geometries used in the abovementioned calculations<sup>24,25</sup> was performed experimentally. An internal check for consistency, including beam integration, was also obtained by comparing the intensities of prominent lines in a given isotope measured with the several geometries used. The accuracy with which the efficiency for the gamma-ray detectors, including uncertainties in the absorber corrections, is known is estimated to be 10% for all the transitions except for the low-energy transition from the first excited states of  $\text{Sm}^{152}$  (122 keV) and of  $\text{Sm}^{154}$  (82 keV). The absorption corrections were very large for the latter, and because of uncertainties in the absorption in the target and in the scattering chamber walls, additional errors of 2% for the 122 keV transition and of 5% for the 82 keV transition must be added to the 10% quoted above. The gamma-ray absorption in the target, target holder, and scattering-chamber wall was determined experimentally using calibration sources. Graded absorbers were used to attenuate the high-intensity radiations from the first excited state and  $K$  x rays which usually dominate a NaI crystal spectrum in Coulomb-excitation experiments. Absorption studies on the graded absorber used immediately in front of the counters were performed with the beam during the course of the experiment.

The inelastically back-scattered ions were detected by an array of 1-cm<sup>2</sup> surface-barrier gold-silicon junction detectors with the sensitive surfaces located in a plane perpendicular to the beam and approximately 1 in. from the target surface (Fig. 2). The detectors were connected in pairs and could all be switched in parallel to obtain a large effective solid angle. As many as 32 detectors were available, although in practice the maximum number used was 20. The advantage of this switching arrangement was that if one of the detectors deteriorated during a long data-accumulation period, it could be switched out without interrupting the experiment. There was no loss in resolution in this procedure and only a slight loss in effective solid angle. The resolution of the whole detector array was 0.34 MeV for

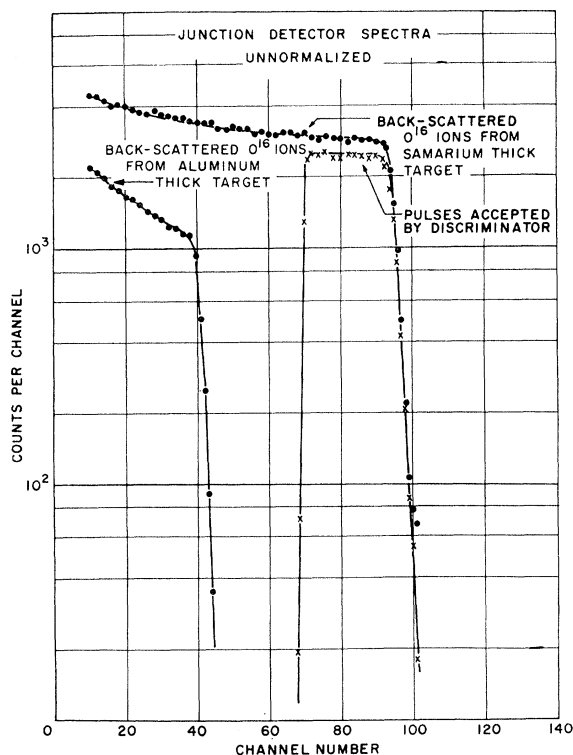


Fig. 3. Particle spectrum for  $\text{O}^{16}$  ions scattered from thick Sm and Al targets. The location of the integral discriminator is indicated by the gated spectrum.

$\alpha$  particles, and the resolution improved almost linearly as the number of counters used was reduced. The detectors subtended an angular range of 132° to 168° relative to the beam direction.

The junction detectors were operated at a bias such that the depletion region was adequate for stopping normally incident 65-MeV oxygen ions, but only normally incident 3-MeV protons or 10-MeV alpha particles. Therefore by choosing an effective discrimination level above 10 MeV, all reactions involving the detection of either a proton or alpha particles could be eliminated from the coincidence spectra. The operational location of the discriminator level in a thick-target particle spectrum, obtained by bombarding  $\text{Sm}^{152}$  with 49-MeV oxygen ions, is shown in Fig. 3. The particle spectrum from an aluminum target is also included for comparison, illustrating that the discriminator level is well above the energy required to exclude all back-scattered particles from low- $Z$  materials. As would be expected, the heavier particles with high energies from the latter reactions scatter predominantly in the forward direction. For the particular discriminator setting shown and the minimum angle defined by the counter array, elastic Coulomb scattering of  $\text{O}^{16}$  can only be detected for nuclei with an atomic number greater than 37.

The discriminator level also defines the effective target thickness used in the thick-target integrations for

<sup>25</sup> S. H. Vegors, L. L. Marsden, and R. L. Heath, Phillips Petroleum Company Report No. IDO-16370, 1958 (unpublished).

<sup>26</sup> R. L. Heath, Phillips Petroleum Company Report No. IDO-16408, 1957 (unpublished).

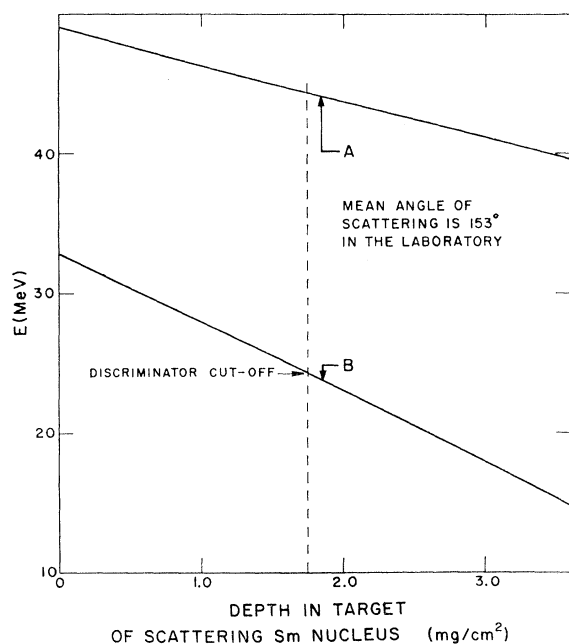


FIG. 4. Illustration of the determination of the effective thickness of the target from the selection of the discriminator cutoff for the particle detectors. Equation (2) was used to calculate the energy loss in the target. Curve A denotes energy of the  $O^{16}$  ion after it has penetrated to the depth of the scattering nucleus. Curve B denotes energy of the  $O^{16}$  ion after it has scattered and emerges from the target at a scattering angle of  $153^\circ$ .

calculating cross sections. The highest energy in the particle spectrum corresponds to the energy of the particle after it elastically scatters from the target surface nuclei. The energy of the incident particle at a depth in the target corresponding to the position of the scattering nucleus, and its energy after it is scattered and emerges from the target have been calculated as a function of the location of the scattering Sm nucleus from the surface. A representative result is illustrated in Fig. 4 for a mean scattering angle of  $153^\circ$ . The position of a typical operating energy discriminator level is indicated. Only particles scattered at a depth from the surface less than the depth corresponding to this discriminator level contribute to gamma-particle coincidences.

The ionization energy loss was obtained from the semiempirical range curves of Hubbard<sup>27</sup> and of Northcliffe<sup>28</sup> for oxygen ions in silver and in gold. A linear extrapolation in nuclear charge was made between silver ( $Z=47$ ) and gold ( $Z=79$ ) to obtain the range of oxygen ions in samarium ( $Z=62$ ). This curve is reproduced to better than 3%, for 8–80-MeV oxygen

ions, by the second-order polynomial,

$$S = 0.000976E^2 + 0.297E + 1.5 \text{ (mg/cm}^2\text{)}, \quad (2)$$

where  $S$  is the range and  $E$  is the energy of the incident ion in MeV. It is clear that  $dE/dS$  does not vary rapidly with energy.

The incident energy for which the thick-target integrations must be terminated is not the energy of the particle corresponding to the discriminator level, but rather the corresponding energy of the particle before it scatters from its target nucleus in the target. Of course, for a finite solid angle subtended by the counters this cutoff energy is not sharp. In order to minimize systematic uncertainties due to the energy-scale calibration and the particle-detector efficiency, an effective integration cutoff energy was determined empirically by comparing the gamma-ray yields from the de-excitation of the first excited state in  $Sm^{148}$  obtained from a total-gamma-ray yield measurement and a coincidence measurement with backscattered particles. The latter measurements were performed with an identical geometry for the gamma-ray detector so that uncertainties regarding the efficiency of this detector are eliminated in this comparison. The absence of any significant population of states in  $Sm^{148}$  other than the first excited state (see Sec. IV) is good evidence that this excitation is expected to be accurately described by perturbation theory, and the largest uncertainty in determining the effective integration cutoff energy comes from determining the gamma-ray intensities. (We have neglected here the consequences of the reorientation effect on calculating the ratio of the two yields.) The error in determining the intensities is small. In extrapolating the cutoff energy thus determined for  $Sm^{148}$  to the other three isotopes under consideration, the dependence of the cutoff on the excitation energy and on the mass of the excited nucleus was taken into account. The gamma-particle coincidence data for all four isotopes were obtained with identical settings for the particle-energy discriminator levels.

In the portion of the experiment performed at the Yale HILAC, a fast slow coincidence system in which provision was made to measure accidental coincidences simultaneously with true coincidences was used for data handling. The continuous simultaneous monitoring of the accidental coincidences was necessitated by the pulsed nature of the accelerator. The true, or accidental, coincidence pulses gated the subdivided memories of several 400-channel analyzers which stored pulse-height information. A variety of slow-coincidence gates, fed by differential single-channel analyzers, were also available in the system, and were used as needed to supply additional selected pulse-height information from counters not being interrogated by the multichannel analyzer. To ensure 100% coincidence efficiency for gamma-ray energies ranging from 50 keV to several MeV, the resolving time  $2\tau$  used was 30 nsec. The total number of true and

<sup>27</sup> E. L. Hubbard, University of California Radiation Laboratory Report No. UCRL-9053, 1960 (unpublished).

<sup>28</sup> L. C. Northcliffe, Nat. Acad. Sci.-Nat. Res. Council Publ. No. 1133 (1956), p. 173.



accidental coincidence pulses, the total number of pulses from each counter, and the number of true and accidental coincidence pulses within each energy interval selected by single-channel differential discriminators, were all recorded on scaling circuits. An arrangement with similar capabilities but using the "crossover coincidence" technique with a somewhat longer resolving time was used during the ORNL phase of this work.

#### IV. RESULTS

In this section the de-excitation spectra from the Coulomb excitation of  $\text{Sm}^{154}$ ,  $\text{Sm}^{152}$ ,  $\text{Sm}^{150}$ , and  $\text{Sm}^{148}$  are presented together with proposed level schemes constructed from these data supplemented by other existing measurements on these nuclei. Spins and parities were not directly measured in the present experiments, and these quantities were inferred from the generic relationship of the Coulomb excited levels to the  $O^+$  ground state as deduced from the excitation multipolarity, transition moments, and the relative population of the excited states as functions of energy and angle of scattering of the projectile. In arriving at a decay scheme, consideration was also given to collective structure systematics when applicable (e.g., rotational bands, and moments of inertia deduced from level spacings) since it is evident from previous work that the states preferentially populated by Coulomb excitation are those associated with collective rotations in the ground-state band, and collective vibrations based on the ground-state configuration.

Use was made of the cascade information obtained from the gamma-gamma coincidence studies. The assignment of gamma rays was facilitated by the association of more than one transition with the de-excitation of a particular level.

The accuracy for the transition energies quoted is  $\pm 1\%$  in this work. All the coincidence spectra shown have been corrected for accidental coincidences which average approximately 10% of the total coincidences. The spectra shown have not had background subtracted.

In the discussion that follows, nomenclature usually appropriate to the description of axially symmetric nuclei will be used. This is simplified for purposes of identification and does not imply that this is necessarily the favored description. In the following subsections, data are presented relevant to each of the samarium isotopes and adequate discussion is given to justify the construction of level diagrams therefrom. We then present data and discussion relevant to the establishment of transition rates in the nuclei studied. We defer until later in the paper the discussion of the level schemes and transition rates *per se*.

##### A. Samarium 154

Prior to the initiation of these measurements, a level in  $\text{Sm}^{154}$  at 82 keV had been established, in Coulomb excitation studies, to be the first excited  $2^+$  state in the

ground-state rotational band. Decay-scheme studies are not available for this nucleus. Additional information on new levels in the ground-state band were communicated by Greenberg *et al.*,<sup>22</sup> based on preliminary measurements associated with this work. Low-lying states in  $\text{Sm}^{154}$  have recently been discussed by de Boer, Goldring, and Winkler,<sup>29</sup> by Kenefick and Sheline,<sup>30</sup> and by Yoshizawa *et al.*<sup>31</sup>

The direct spectrum taken at a bombarding energy of 49 MeV, shown in Fig. 5(a), reveals no strong transitions other than the four transitions assigned to the de-excitation of members of the ground-state band, indicating that the vibrational bands in this nucleus lie moderately high in energy and are not readily excited in Coulomb excitation. The background discussed earlier tends to obscure the very weakly excited lines in the direct spectra. The energies of the four ground-state band transitions are 82 keV ( $2^+ \rightarrow 0$ ), 185 keV ( $4^+ \rightarrow 2^+$ ), 278 keV ( $6^+ \rightarrow 4^+$ ), and 360 keV ( $8^+ \rightarrow 6^+$ ), three of which show up prominently in Fig. 5(a). The 360-keV gamma ray only appears as a shoulder in this spectrum, and the only other significantly strong gamma ray is the 511-keV annihilation radiation. The latter appeared in all the direct and gamma-gamma coincidence spectra taken, and its strength is an indication of degree of surface contamination of the target by oil vapors and oxides. The cascade nature of the four Coulomb excitation gamma rays was established in the three gamma-gamma coincidence spectra shown in Figs. 5(b), 5(c), and 5(d). The differential energy gates chosen for these measurements are illustrated in Fig. 5(e).

Further corroboration for these assignments was obtained by comparing the relative intensities of the four gamma rays in the direct spectrum with the relative intensities in the gamma-particle coincidence spectrum shown in Fig. 5(f). The enhancement in the population of the higher spin states, when large angle scatterings are selected, is evident. This behavior is predicted by multiple-Coulomb-excitation theory<sup>32-34</sup> for members of the ground-state band. A quantitative comparison showing quite good agreement with experiment is discussed in Sec. V. The 360-keV transition may be identified clearly in the gamma-particle spectrum, and the background is very significantly reduced as is clear from the absence of the 511-keV gamma ray and a general emergence of weak transitions which did not appear above background in the corresponding direct spectrum.

<sup>29</sup> J. de Boer, G. Goldring, and H. Winkler, *Phys. Rev.* **134**, B1032 (1964).

<sup>30</sup> R. A. Kenefick and R. K. Sheline, *Phys. Rev.* **135**, 939 (1964).

<sup>31</sup> Y. Yoshizawa, B. Elbek, B. Herskind, and M. C. Olesen, *Nucl. Phys.* **73**, 273 (1965).

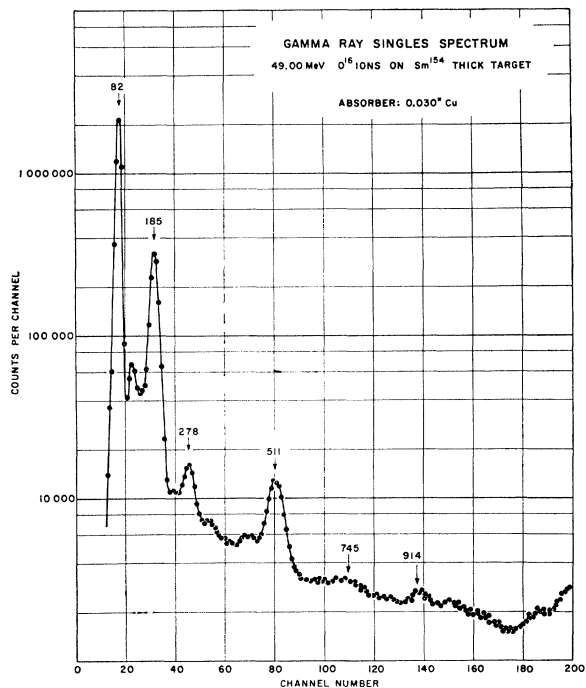
<sup>32</sup> K. Alder and A. Winther, *Kgl. Danske Videnskab. Selskab, Mat. Fys. Medd.* **32**, No. 8 (1960).

<sup>33</sup> K. Alder, *Proceedings of the Third Conference on Reactions Between Complex Nuclei*, edited by Albert Ghiorso, R. M. Diamond, and H. E. Conzett (University of California Press, Berkeley, California, 1963).

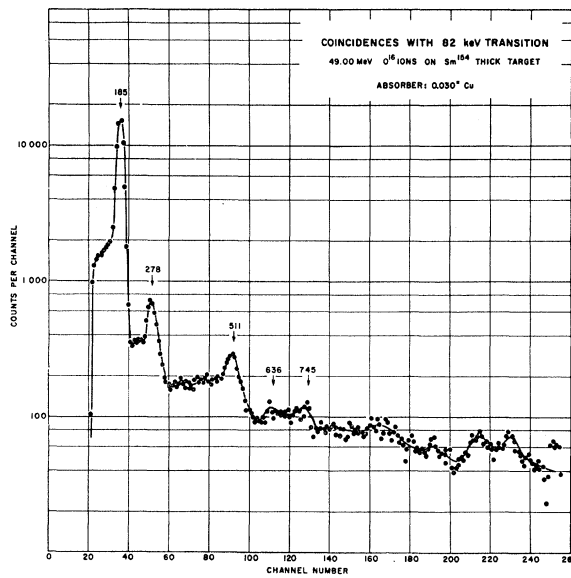
<sup>34</sup> I. Berson, *Nucl. Phys.* **67**, 296 (1965).

The energy reported here for the  $6^+ \rightarrow 4^+$  transition is somewhat lower than that of 284 keV obtained by de Boer *et al.*,<sup>29</sup> and of 282 keV obtained by Kenefick and Sheline.<sup>30</sup> A larger disagreement seems to exist between

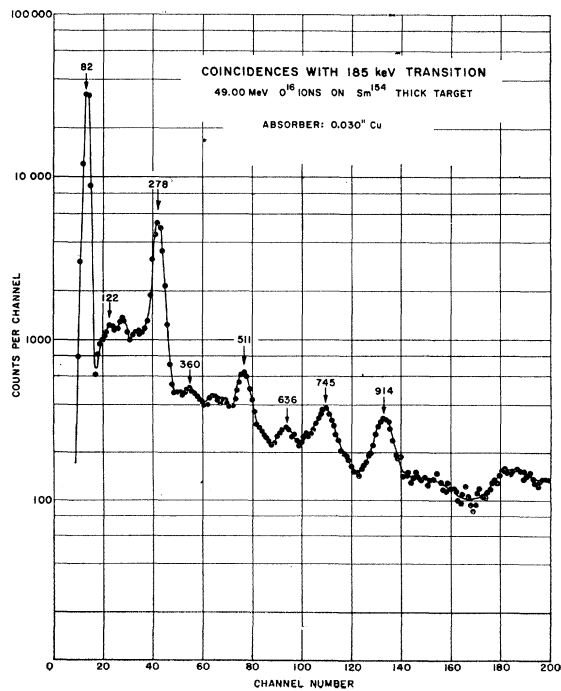
the 360-keV energy assigned to the  $8^+ \rightarrow 6^+$  transition by this experiment and an energy of 401 keV reported by de Boer *et al.*<sup>29</sup> A recent remeasurement of these two transitions using a Ge(Li) detector is in agreement with



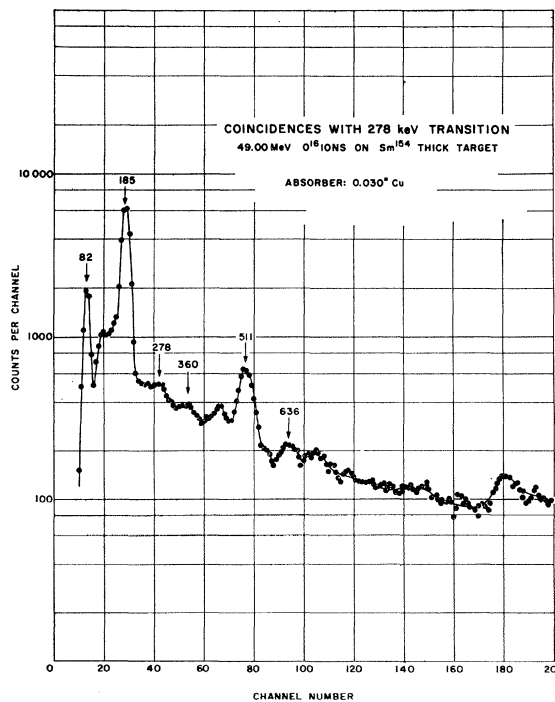
(a)



(b)



(c)



(d)

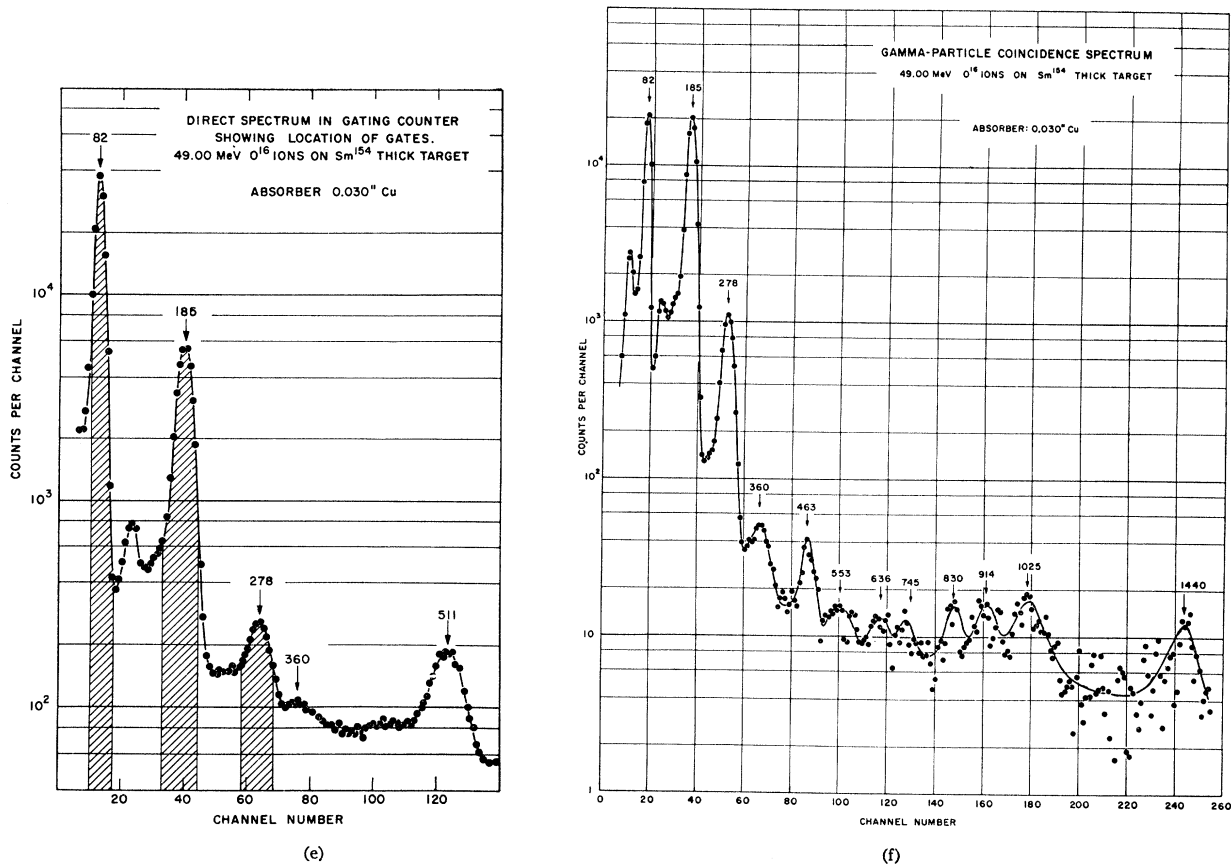


FIG. 5. Gamma-ray spectra obtained from 49-MeV  $\text{O}^{16}$  ions on  $\text{Sm}^{154}$ ; (a) direct singles spectrum; (b), (c), (d) spectra taken in coincidence with the 82 keV ( $2^+ \rightarrow 0^+$ ), 185 keV ( $4^+ \rightarrow 2^+$ ), and 278 keV ( $6^+ \rightarrow 4^+$ ) transitions in the ground-state band; (e) gates selected for the gamma-gamma coincidence measurements; (f) gamma-particle coincidence spectrum. Energies are in keV.

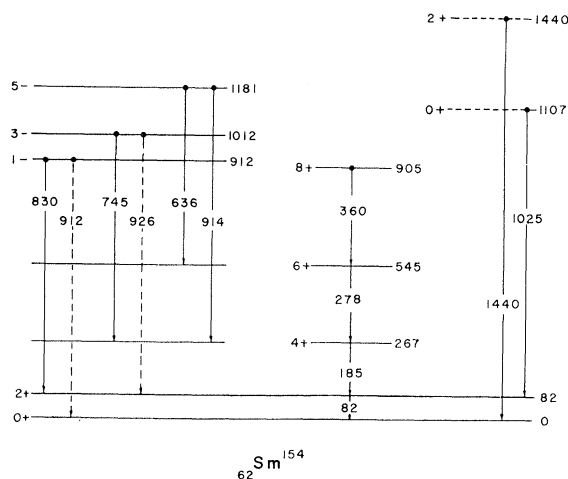
assignments reported here. The 185-keV transition has also been studied by Graetzer and Bernstein.<sup>35</sup>

It has already been indicated that the gamma-particle spectrum shows weak transitions at 463, 553, 636, 745, 830, 914, 1025, and approximately 1440 keV. The 463-keV peak is most probably a sum coincidence, since its intensity is very close to the 3.5% of the 278-keV intensity predicted from the known detection efficiency of the gamma-ray detector. No assignment has been made for the rather broad peak centered at 553 keV. It does not appear with any appreciable intensity in any other coincidence spectrum.

The next four higher energy transitions have been associated with the de-excitation of three members of an odd-parity band. The gamma-gamma coincidence spectra show that the 636-keV gamma ray is in coincidence with the transition from the  $6^+$  member of the ground-state band, while the 745- and 914-keV transitions feed the  $4^+$  state in the ground-state band. If transition multiplicities not greater than quadrupole are assumed, then the 636-keV transition must originate from

a state with a spin no smaller than 4, and the 745-keV and 914-keV transitions must de-excite states with spins 2 or greater. A  $2^+$  level at  $267+745=1012$  keV associated either with a gamma or beta band would be expected to produce stronger transitions to the  $2^+$  level in the ground-state band. Such strong transitions are common for nuclei in this region as is particularly evident in  $\text{Sm}^{152}$  to be discussed below. None appear either in the  $\text{Sm}^{154}$  direct spectrum or in the spectrum in which coincidences are taken with the 82-keV transition. A  $4^+$  level associated with any one of these three transitions is also unlikely since no  $2^+$  level is observed which would be preferentially populated by Coulomb excitation. A consistent interpretation of the data can be obtained on the assumption of a  $3^-$  level at 1012 keV and a  $5^-$  level at 1181 keV as shown in the proposed decay scheme in Fig. 6. The 830-keV transition found in the gamma-particle spectrum has been tentatively attributed to the de-excitation of a  $1^-$  state to the ground-state  $2^+$  state. The three odd-parity states then form the rotational sequence associated with an octupole vibrational band and its indicated moment of inertia is consistent with that of other octupole bands found in the deformed

<sup>35</sup> R. Graetzer and E. M. Bernstein, Phys. Rev. **129**, 1772 (1963).

FIG. 6. Level scheme for  $\text{Sm}^{154}$ .

region at  $150 < A < 190$ . The position of the band head is also typical of this region.

It may be pointed out that arguing from multiple-Coulomb-excitation theory, the 830-keV transition, as well as transitions from the  $5^-$  level, are expected to be enhanced relative to transitions from the  $3^-$  level when particles scattered in the backward direction are detected in coincidence. The predicted relative populations of the three states, assuming that they are members of an octupole band, have been calculated from multiple-Coulomb-excitation theory by Lutken and Winther<sup>36</sup> (see result for  $\text{Sm}^{152}$  Fig. 10). A number of approximations go into this calculation; these are discussed in Sec. V. However, the qualitative features are not expected to be affected by them. The expected enhancement in the populations of the  $1^-$  and  $5^-$  states relative to the  $3^-$  when scattered particles are selected in the backward cone is represented by the data.

Further evidence for the collective character of these states can be inferred from the measured reduced transition probability from the ground state which was found to have a lower limit of 11 single-particle units (see Sec. IV). Hansen and Nathan<sup>37</sup> have reported the strong Coulomb excitations, with  $\alpha$  particles, of a level complex at 1010 keV, a large part of which they attribute to a  $3^-$  level at that energy on the basis of the observed angular correlation of the decay gamma ray with respect to the backscattered  $\alpha$  particles. Kenefick and Sheline<sup>30</sup> also observe a strong excitation of a level at 1014 keV using the  $(p, p')$  reaction. These have been identified with the 1012-keV  $3^-$  level deduced from the present measurements.

Two gamma rays (at 1025 keV and 1440 keV) remain to be considered. Considering their high energy, these are excited relatively strongly in the gamma-particle

coincidence spectrum, and are most probably associated with the decay of states in the beta or gamma vibrational bands. Some guidance here may be obtained from a study by Bès<sup>38</sup> on the location of beta- and gamma-band heads for nuclei in this region. His calculations favor that the lower energy be associated with the beta band,  $\sim 1200$  keV, with the lowest gamma vibrational state predicted at  $\sim 1500$  keV. It should be noted, however, that the excitation energy of the beta and gamma vibrations vary very rapidly near the boundaries of the deformed region and any such conclusions are at best qualitative. In  $\text{Sm}^{152}$ , where the beta and gamma vibrational states have been conclusively identified (see below), the strongest transition from the beta band to the ground state occurs for  $0^+ \rightarrow 2^+$ . If we assume that the 1025-keV transition is the analog of this transition in  $\text{Sm}^{154}$ , this places the  $0^+$  beta-band head at 1107 keV. Multiple-Coulomb excitation calculations favor this interpretation (see Fig. 8). Kenefick and Sheline<sup>30</sup> have reported a level at 1104 keV which they have assigned as the  $2^+$  state in the beta band. The background in the 82-keV gamma-gamma coincidence spectrum is too large to make a definite choice between these two assignments.

Similarly, following the pattern displayed by the de-excitation of the  $2^+$  gamma vibrational level in  $\text{Sm}^{152}$  which decays with comparable intensities to the  $2^+$  and  $0^+$  levels of the ground-state band, we may expect the  $2^+$  level of the gamma vibrational band to be either at 1440 or 1522 keV. Kenefick and Sheline<sup>30</sup> see a strong excitation at 1444 keV which they identify as the  $2^+$  level. There is no definite evidence in the present gamma-particle spectrum for a line at an energy of  $1444 - 82 = 1362$  keV which would be expected from the de-excitation of a  $K=2, I=2^+$  level at 1444 keV, although the broad enhancement in this region of the gamma-particle coincidence spectrum could certainly include such a transition.

The energy-level scheme shown in Fig. 6 substantially agrees with the results obtained from Coulomb-excitation measurements with 43.5 MeV  $\text{O}^{16}$  ions carried out concurrently with this work by Yoshizawa *et al.*<sup>31</sup> The conclusions in the latter investigations were based principally on gamma-particle coincidence measurements and did not include gamma-gamma coincidence data.

### B. Samarium 152

Gamma-ray transitions have been observed in previous work, principally in beta-decay studies, at energies of 122, 245, 563, 841, 963, 965, 1087, and 1114 keV.<sup>39-41</sup> All of these have been confirmed in this work. In addition, the previous assignment of levels in the ground-state, beta-vibration, gamma-vibration, and octupole

<sup>36</sup> R. Lutken and A. Winther, Kgl. Danske Videnskab. Selskab, Mat. Fys. Medd. 2, No. 6 (1964).

<sup>37</sup> D. Hansen and O. Nathan, Nucl. Phys. 42, 197 (1962).

<sup>38</sup> D. R. Bès, Nucl. Phys. 49, 544 (1963).

<sup>39</sup> O. Nathan and M. A. Waggoner, Nucl. Phys. 2, 548 (1957).

<sup>40</sup> O. Nathan and S. Hultberg, Nucl. Phys. 10, 118 (1959).

<sup>41</sup> L. Grodzins, Phys. Rev. 109, 1015 (1958).

bands have been extended to include higher spin members in each of these bands.<sup>22,23,42</sup> Information on levels in Sm<sup>152</sup> has recently been reported from ( $p,p'$ ) studies,<sup>30</sup> and from the above mentioned Coulomb excitation measurements by Yoshizawa *et al.*<sup>31</sup> Most of the radiations mentioned above appear in the direct spectrum shown in Fig. 7(a) measured with 49-MeV O<sup>16</sup> ions. Direct gamma-ray spectra were also taken at incident energies of 16, 36.5, 45, 51.7, 57, and 64 MeV to trace the energy dependence of the population of levels in the higher lying bands. The low-intensity peak at 82 keV in Fig. 7(a) originates from a small Sm<sup>154</sup> target impurity. As was the case for Sm<sup>154</sup>, the 511-keV gamma ray and gamma rays above 1100 MeV arise from target surface contamination.

The ground-state rotational band has well-established 2<sup>+</sup> and 4<sup>+</sup> levels at 121.8 and 366.6 keV. Transitions at 122 and 245 keV from these levels are very prominent in all the direct and coincidence spectra shown in Figs. 7(a)–7(d). The reduction in the 122-keV gamma-ray intensity relative to that of the 245-keV gamma ray is due to the absorber used during accumulation of these spectra. The 340-keV gamma ray, which appears strongly in nearly all spectra, and is in coincidence with these two ground-state band transitions, has been assigned in an earlier communication<sup>22</sup> to the 6<sup>+</sup> → 4<sup>+</sup> transition in the ground-state band. This assignment has been further justified by comparison of the three gamma-ray experimental intensities (in the spectrum obtained when gamma rays were taken in coincidence with backscattered particles) with the intensities predicted from multiple-Coulomb-excitation theory. Studies at different ion bombarding energies also showed the predicted behavior for excitation of these three ground-state band members. Some evidence has also been obtained for the excitation of the 8<sup>+</sup> state of this band in studies at higher bombarding energies. The 8<sup>+</sup> → 6<sup>+</sup> transition was not completely resolved in the NaI spectra taken because of the complexity of these spectra at higher incident ion energies, but later observations with a Ge(Li) semiconductor detector indicated a transition with approximately the correct intensity at an energy of approximately 480 keV. This transition could not be confirmed in any of the coincidence measurements for reasons already mentioned.

Six of the observed gamma-ray transitions were associated with the de-excitation of the 2<sup>+</sup>, 3<sup>+</sup>, and 4<sup>+</sup> levels in the gamma-vibrational band. The 2<sup>+</sup> band-head level de-excites via a 965-keV transition to the 2<sup>+</sup> ground-state band member and also, with a relatively strong transition of 1087 keV, directly to the ground state. Both these transitions have been shown to be predominately E2 in character.

Evidence for excitation of the 3<sup>+</sup> state was obtained from the gamma-gamma coincidence measurements in-

volving the decay of the first and second excited states in the ground-state band and from measurements of direct spectra carried out at higher bombarding energy.<sup>12</sup> The apparent strength with which the 3<sup>+</sup> level is excited exceeds the multiple-excitation-theory prediction by approximately a factor of 2. This presently is not understood fully, but certainly depends critically on the approximations used in the multiple-Coulomb-excitation calculations. There is also some uncertainty associated with the possible presence of a background radiation at approximately 850 keV, unresolved from the 869-keV radiation which de-excites the 3<sup>+</sup> level, which may account for the apparently large anomalous population of the 3<sup>+</sup> state.

The 1260-keV gamma ray, observed in the gamma-particle coincidence spectrum, [Fig. 7(f)] and the weak 1016-keV line, seen in coincidence with transitions from the 4<sup>+</sup> state in the ground-state band [Fig. (7c)], have been interpreted as originating from the de-excitation of a 4<sup>+</sup> level in the gamma-vibrational band. The energy spacing between the 4<sup>+</sup> and 3<sup>+</sup> levels is in reasonable accord with the moment of inertia calculated from the 2<sup>+</sup> to 3<sup>+</sup> energy spacing. The 1260-keV transition was quoted in a preliminary report of the earlier series of experiments, referred to previously, as at 1273 keV. This difference in energy has been found to reflect an error in the energy scale of the earlier experiments.

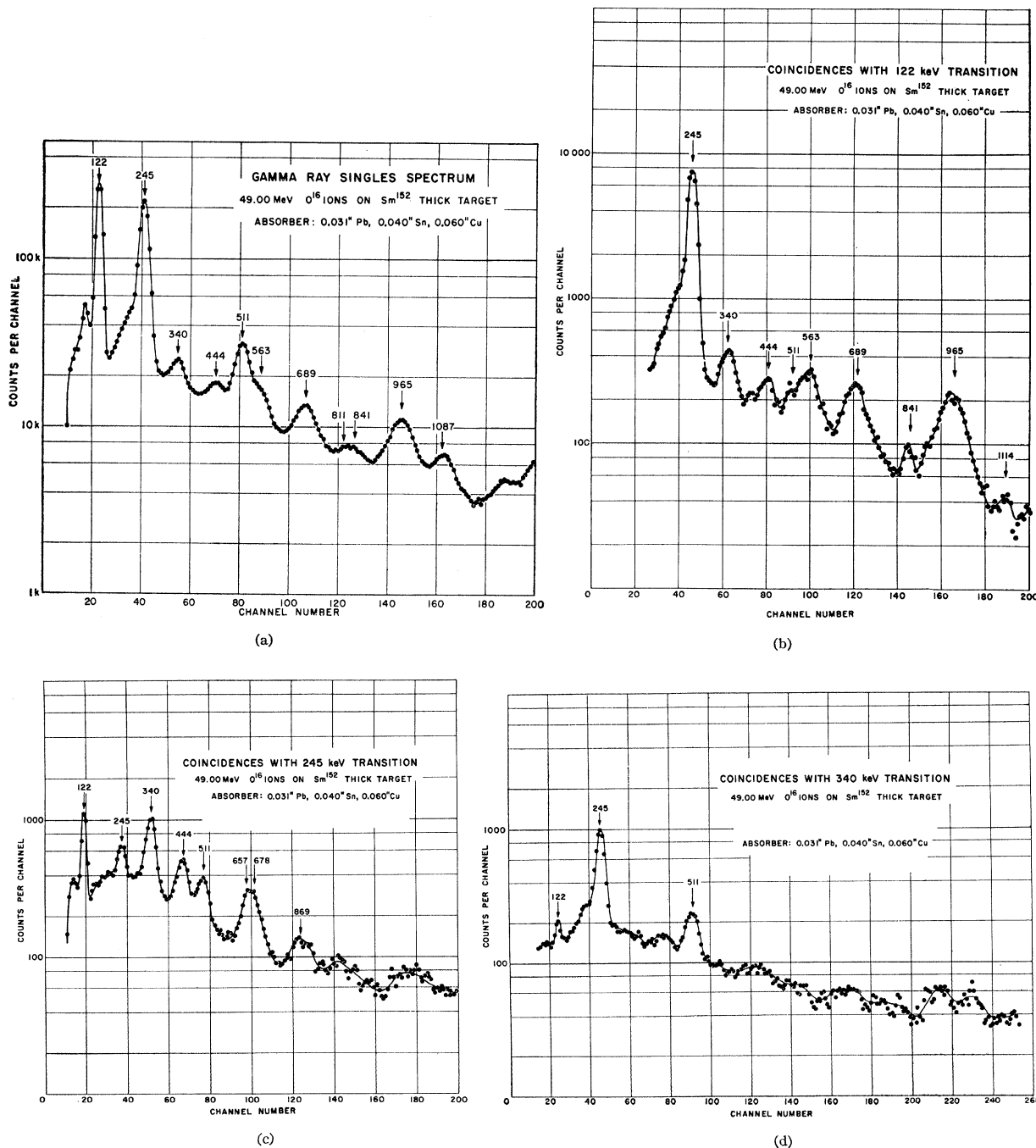
The beta-vibrational excitations appear at a relatively low energy in this nucleus, and in consequence, several of the levels in this band are strongly populated in these studies. A consistent interpretation of the information obtained from the direct and coincidence spectra places the 0<sup>+</sup> level at 685 keV and the 2<sup>+</sup> level at 811 keV. The 0<sup>+</sup> state de-excites principally through a 563-keV transition to the 2<sup>+</sup> member of the ground-state band. It appears as a shoulder on the 511 annihilation radiation peak in the direct spectrum, but is well resolved in gamma-gamma coincidences with the 122-keV ground-state transition, and in the gamma-particle coincidence spectrum. The 2<sup>+</sup> level is depopulated by 444-, 689-, and 811-keV transitions to the 4<sup>+</sup>, 2<sup>+</sup>, and 0<sup>+</sup> states, respectively, in the ground-state band. The former two appear very distinctly in all spectra taken, while the latter is very weak and its intensity could only be determined approximately.

The excitation of the 0<sup>+</sup> level was identified by at least two methods. The calculated behavior of both the total cross section with energy and the differential cross section with the angle of the scattered particle is very distinctive for this state. For the former the scattered particle is not detected; for the latter, gamma rays are detected in coincidence with the inelastically scattered particles at a particular particle scattering angle  $\theta$ . The predictions for the differential cross section, based on the available multiple-Coulomb-excitation calculations without any consideration of interband mixing,<sup>36</sup> are displayed in Fig. 8. A prominent feature of the total

<sup>42</sup> G. G. Seaman, J. S. Greenberg, D. A. Bromley, and F. K. McGowan, *Bull. Am. Phys. Soc.* **9**, 108 (1964).

cross section is the rather rapid decrease, with incident energy, in the ratio of the cross sections for the excitation of the  $2^+$  and  $0^+$  states.<sup>33</sup> In the differential cross section this ratio is expected to be smaller than unity for backward scatterings and much larger than unity for forward scatterings. Both of these predictions were borne out by the data. The behavior with incident ion energy of the total cross section for this state has been published elsewhere.<sup>12</sup> The large enhancement of

the 563-keV transition intensity over that of the 444-keV and the 689-keV transitions from the  $2^+$  state in the gamma-particle coincidence spectrum dramatically illustrates the expected characteristic behavior of the differential cross section when a comparison is made with the relative intensities of these gamma rays in the direct spectrum. It may be noted that the predicted enhancement, as shown in Fig. 8, differs somewhat from the measured one most probably because of the effect of



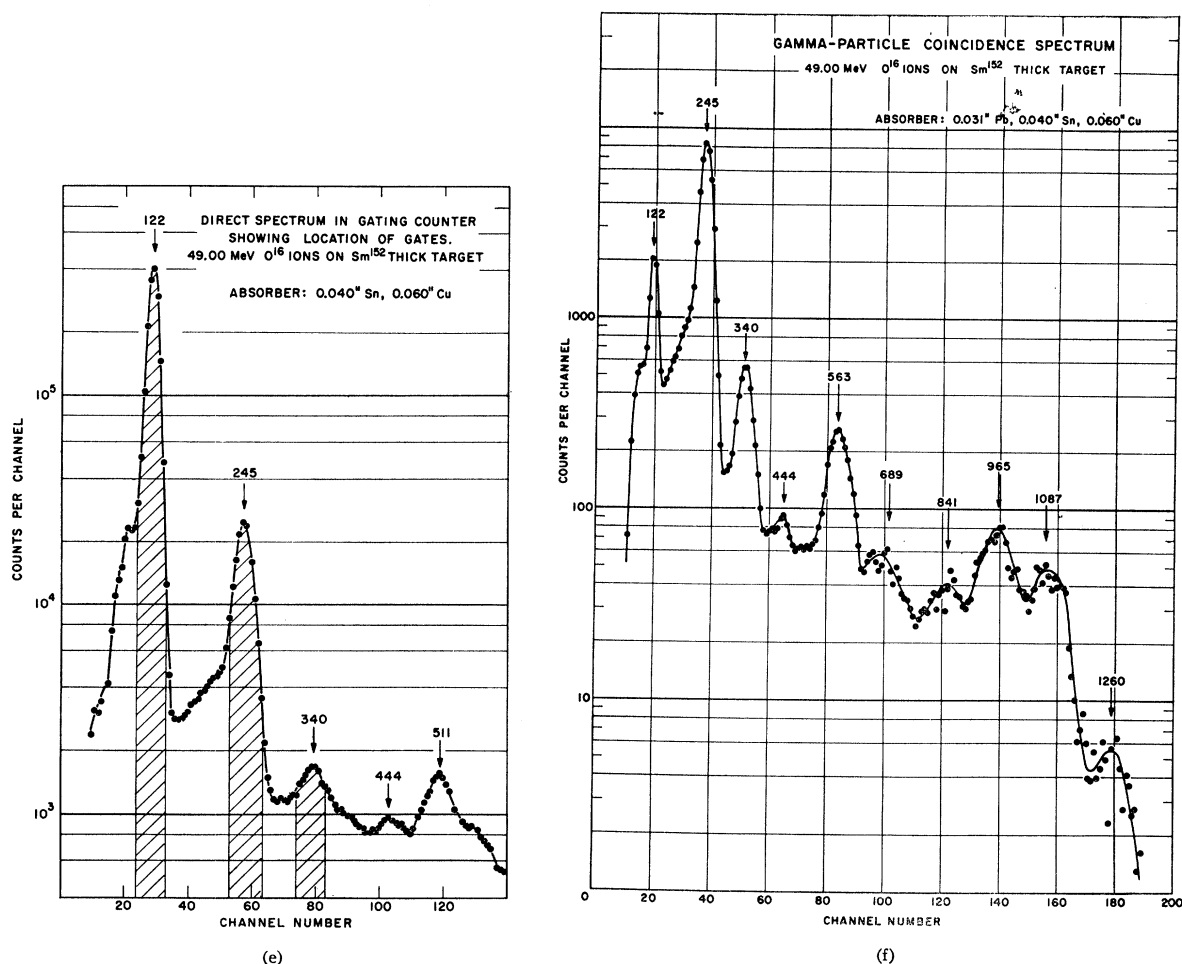


FIG. 7. Gamma-ray spectra obtained for 49-MeV  $O^{16}$  ions on  $Sm^{152}$ ; (a) direct singles spectrum; (b), (c), (d) spectra taken in coincidence with the 122 keV ( $2^+ \rightarrow 0$ ), 245 keV ( $4^+ \rightarrow 2^+$ ), 340 keV ( $6^+ \rightarrow 4^+$ ) transitions in the ground-state band; (e) gates selected for the gamma-gamma coincidence measurements; (f) gamma-particle coincidence spectrum.

interband mixing on the excitation probability for the  $2^+$  state. This latter point is discussed in Sec. V.

Further data relevant to the excitation of the  $0^+$  state was obtained from an internal-conversion-electron spectrum taken with a specially designed, broad-range spectrometer.<sup>43</sup> The very intense monopole transition to the ground state appears very distinctly in this spectrum (Fig. 9), as do the other transitions already mentioned. The prominent line at 412 keV has not yet been identified.

The situation regarding the  $4^+$  beta-vibrational state is less certain reflecting a near degeneracy in level excitation energy with that of an odd-parity  $3^-$  octupole state. Evidence for a  $3^-$  state at 1070 keV has been reported by Hansen and Nathan<sup>37</sup> using inelastic alpha-particle scattering near the Coulomb barrier. The transition these authors observe, however, may be composite,

with some contribution from the 1087 keV,  $2^+$  gamma-vibrational state. Kenefick and Sheline<sup>30</sup> have observed a strongly populated level at 1042 keV in ( $pp'$ ) scattering which they assign as the  $3^-$  state. In both these experiments it is expected that excitation of the octupole state would compete very favorably with excitation of the even-parity states. For Coulomb excitation induced by heavy ions, on the other hand, the quadrupole transitions are expected to be dominant.

If excited, both the  $3^-$  and  $4^+$  states can decay, by a dipole and quadrupole transition, respectively, to the  $4^+$  state in the ground-state band. The strong composite line centered on 670 keV in the gamma-gamma coincidence spectrum [Fig. 7(c)] probably contains both these de-excitations. Although it is not possible to decompose this line unambiguously, nor to determine from it the individual transition energies and the order with which they are to be assigned, some further information can be obtained from the different population of the  $3^-$  and  $4^+$  states with scattering angle. Figure 10 shows the

<sup>43</sup> G. A. Burginyon and J. S. Greenberg, Nucl. Instr. Methods 41, 109 (1966).

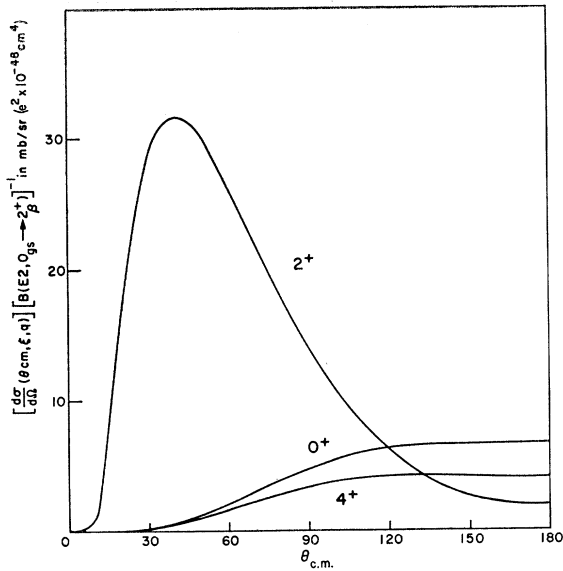


FIG. 8. Differential cross sections for the multiple Coulomb excitation of the beta-band levels in  $\text{Sm}^{152}$  expressed in units of the quadrupole reduced transition probability from the ground state to the  $2^+$  member of the beta band.  $B(E2, 0_{gs}^+ \rightarrow 2_{\beta}^+)$  is in units of  $e^2 \times (10^{-48} \text{ cm}^4)$ . The excitation parameters are  $q=1.548$  and  $\xi=0.435$ . The latter are average values for a bombarding energy of 49 MeV and a thick-target cutoff energy as specified in the text. In this figure  $\theta_{\text{c.m.}}$  is the angle of scattering of the incident ion in the center-of-mass system.

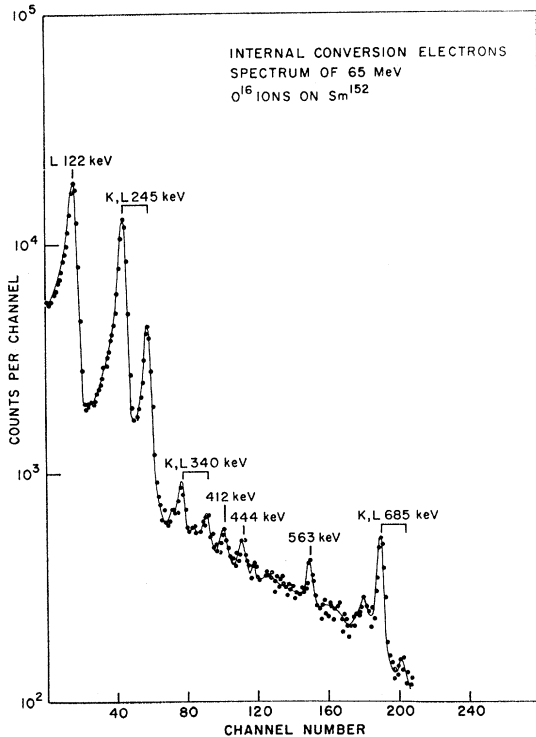


FIG. 9. Spectrum of internal conversion electrons from the de-excitation of levels in  $\text{Sm}^{152}$  after bombardment by 65-MeV  $\text{O}^{16}$  ions showing the prominent internal conversion line from the  $0^+ \rightarrow 0^+$  beta band to ground-state transition.

calculated preference for forward scattering in the excitation of a  $3^-$  state in an octupole band. It was assumed for this calculation that the intraband transition moment was equal to that of the ground-state band. This predicted dependence on scattering angle is to be compared with the predicted rise in cross section for backward angles for the case of a  $4^+$  beta-vibrational-state excitation.

The gamma-particle spectrum shows a broadening of the 689-keV line on its low-energy side, implying that the lower energy transition involved in the composite line, centered at 670 keV in Fig. 7(c), should be identified with the de-excitation of the  $4^+$  state. In addition, a direct spectrum taken with a Ge(Li) detector showed a

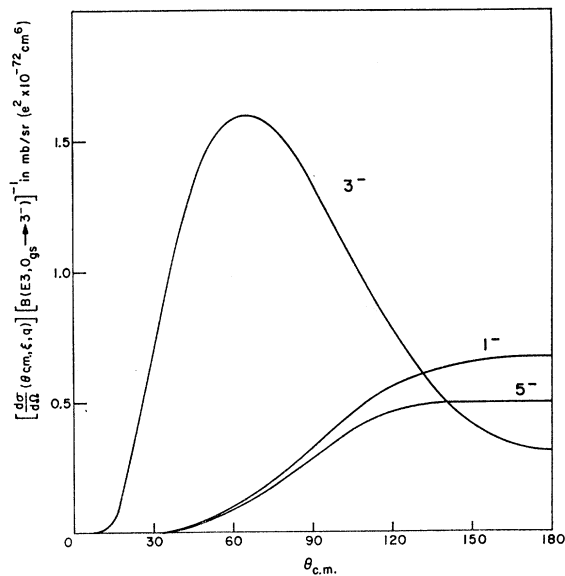
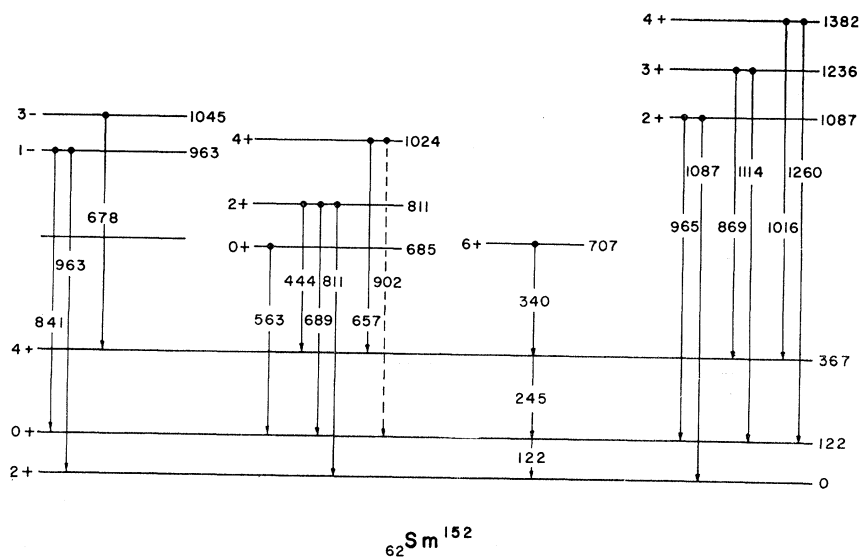


FIG. 10. Differential cross sections for the multiple Coulomb excitation of the octupole band levels in  $\text{Sm}^{152}$  expressed in units of the octupole reduced transition probability from the ground state to the  $3^-$  member of the octupole band.  $B(E3, 0_{gs}^+ \rightarrow 3^-)$  is in units of  $e^2 \times (10^{-72} \text{ cm}^6)$ . The excitation parameters are  $q=1.548$  and  $\xi=0.563$ . The latter are average values for a bombarding energy of 49 MeV and a thick-target cutoff energy as specified in the text. In this figure  $\theta_{\text{c.m.}}$  is the angle of scattering of the incident ion in the center-of-mass system.

transition at 657 keV clearly resolved from another broadened line near 689 keV. These considerations together suggest that the  $4^+$  level is probably located at 1024 keV and the  $3^-$  level at approximately 1045 keV, the latter assignment being in agreement with the  $(pp')$  measurements quoted above.<sup>30</sup> In the earlier communication of these results, based on the preliminary information available at that time, these assignments were reversed. It may also be noted that if half the intensity in the 670-keV line is associated with the de-excitation of the  $3^-$  state, and if the Alaga branching rules<sup>44</sup> are used to estimate the other mode of decay to

<sup>44</sup> G. Alaga, K. Alder, A. Bohr, and B. R. Mottelson, *Kgl. Danske Videnskab. Selskab, Mat. Fys. Medd.* **29**, No. 9 (1955).



FIG. 11. Level scheme for  $\text{Sm}^{152}$ .

the  $2^+$  state in the ground-state band, an octupole reduced transition probability of 15 single-particle units is obtained for this transition. This transition strength agrees very well with the octupole strengths found in the other Sm isotopes studied.

Evidence for a  $1^-$  state at 963 keV, previously studied in the decay of  $\text{Eu}^{152}$ , was also obtained. The 841-keV dipole transition from this  $1^-$  to the  $2^+$  state in the ground-state band is weak and appears most clearly in the spectrum taken in coincidence with the 122-keV line and in the gamma-particle spectrum. The 963-keV transition to the ground state is obscured by the strong 965-keV gamma ray from the  $2^+$  gamma-vibrational state.

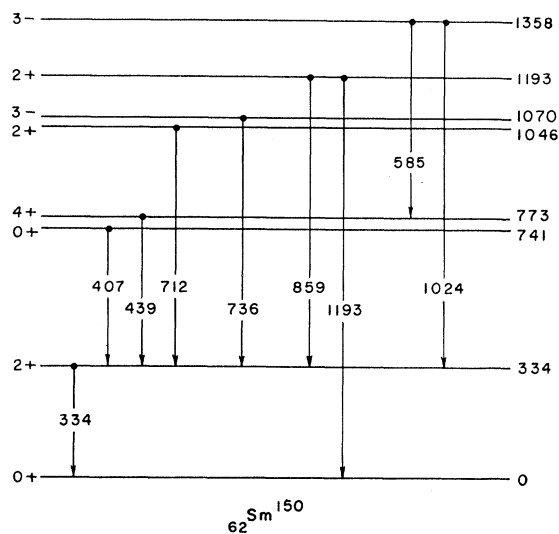
The energy-level scheme for  $\text{Sm}^{152}$  inferred from the above results and discussions is shown in Fig. 11.

### C. Samarium 150

A departure from a rotational level structure for  $\text{Sm}^{150}$  is apparent in Fig. 12, which was constructed from measurements to be reported herein and from the results of other investigations cited below. Again, as in the cases of  $\text{Sm}^{154}$  and  $\text{Sm}^{152}$ , levels which are connected to the ground state with large quadrupole transition moments were primarily accessible to investigation.

The excited states in  $\text{Sm}^{150}$  have been studied using a variety of methods. The decay of  $\text{Eu}^{150}$  and of  $\text{Eu}^{150m}$  have been investigated by Harmatz *et al.*,<sup>45</sup> Yoshizawa *et al.*,<sup>46</sup> Guttman *et al.*,<sup>47</sup> and by Ricci *et al.*<sup>48</sup> Extensive thermal-neutron gamma-ray studies have been performed by Groshev *et al.*,<sup>49</sup> Smithers *et al.*,<sup>50</sup> and by

Bieber *et al.*<sup>51</sup> Recently a large number of levels have been identified and classified in energy in studies of ( $d,p$ ) and ( $p,p'$ ) reactions<sup>52</sup>; Coulomb excitation, by alpha particles,<sup>53</sup> of levels at 335 ( $2^+$ ) keV, at approximately 770 keV and at 1074 ( $3^-$ ) keV has been reported. Spin assignments have been made most directly through directional correlation experiments by Guttman *et al.*, and by Smithers *et al.* Although some detailed disagreement exists in these various investigations, there is substantial agreement on the energies and spin assignments of the following excited states below 1400 keV: 334 ( $2^+$ ), 741 ( $0^+$ ), 773 ( $4^+$ ), 1046 ( $2^+$ ), 1070 ( $3^-$ ), 1166 ( $2^+$ ),

FIG. 12. Level scheme for  $\text{Sm}^{150}$ .

<sup>45</sup> B. Harmatz, T. H. Handley, and J. W. Mihelich, Phys. Rev. **123**, 1758 (1961).

<sup>46</sup> Y. Yoshizawa *et al.*, Nucl. Phys. **46**, 78 (1963).

<sup>47</sup> M. Guttman *et al.*, Bull. Am. Phys. Soc. **6**, 429 (1961).

<sup>48</sup> R. A. Ricci *et al.*, Nucl. Phys. **32**, 490 (1962).

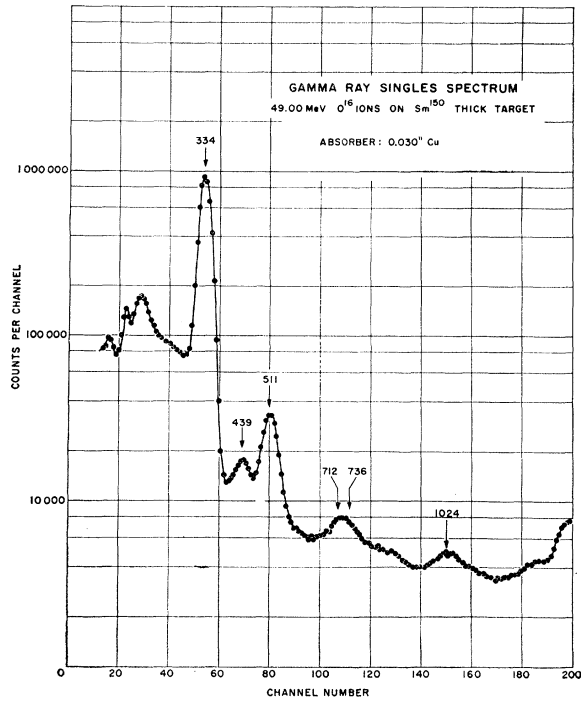
<sup>49</sup> L. V. Groshev *et al.*, Nucl. Phys. **43**, 683 (1963).

<sup>50</sup> R. K. Smithers *et al.*, Bull. Am. Phys. Soc. **7**, 316 (1962).

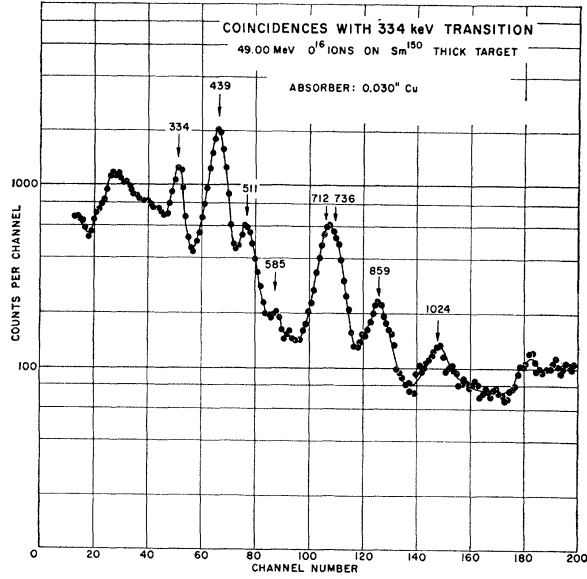
<sup>51</sup> E. Bieber *et al.*, Z. Physik **170**, 465 (1962).

<sup>52</sup> R. A. Kenefick and R. K. Shelton, Phys. Rev. **133**, B25 (1964).

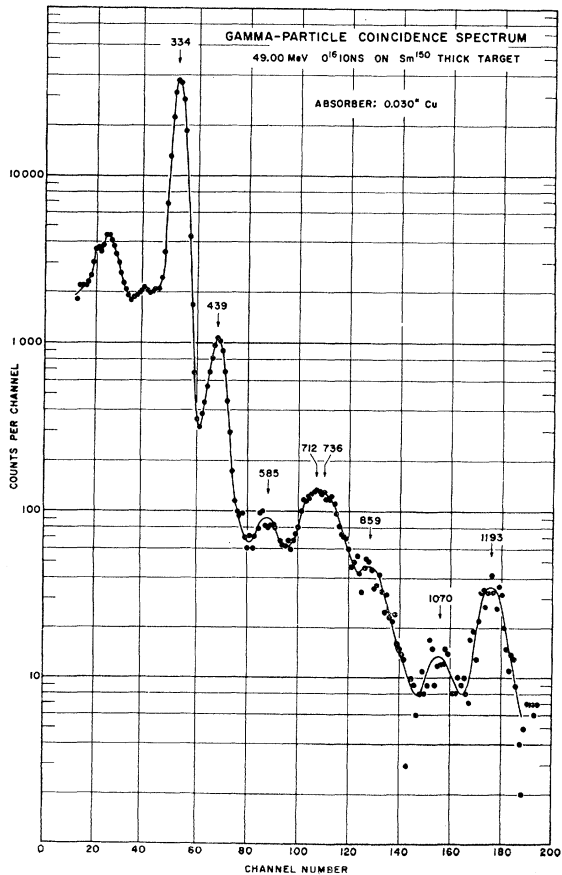
<sup>53</sup> O. Nathan and V. Popov, Nucl. Phys. **21**, 631 (1961).



(a)



(c)



(b)

FIG. 13. Gamma-ray spectra obtained from 49-MeV  $O^{16}$  ions on  $Sm^{150}$ : (a) direct singles spectrum; (b) gamma-particle coincidence spectrum; (c) spectrum taken in coincidence with the 334-keV ( $2^+ \rightarrow 0^+$ ) transition.

1280, and 1358(3<sup>-</sup>) keV. Except for the 1166- and 1280-keV states all of these have been observed in the present experiment.

A strong 334-keV transition occurs both in the direct and in the gamma-particle coincidence spectra. The transition quadrupole moments obtained from both these spectra agree very well with each other and with the previously measured value. The 407- and 439-keV de-excitations from the 0<sup>+</sup> and 4<sup>+</sup> states at 741 and 773 keV, respectively, are not resolved in any of the NaI spectra. They were resolved, however, in a direct spectrum taken with a Ge(Li) detector and in an internal conversion spectrum obtained with the spectrometer mentioned previously. As in the case of the previous two nuclei, the apparent multiple excitation of these two states in Sm<sup>150</sup> is greatly enhanced when coincidences are taken with the backscattered heavy ions. This enhancement is clearly apparent in a comparison between the gamma-particle spectrum, shown in Fig. 13(b), and the direct spectrum in Fig. 13(a). Coincidences taken with the 334-keV gamma-ray transition verify that the 439-keV line is in cascade with the latter. Although no direct measurement was made of the spins of these two states, their relative population is in quite good agreement with the predicted Coulomb excitation of two harmonic vibrations of 0<sup>+</sup> and 4<sup>+</sup> character. (See Sec. V for further discussion.)

Gamma-gamma coincidences taken with the 334-keV transition [Fig. 13(c)] further show that gamma rays with energies 583, 712, 736, 859, and 1024 keV occur in cascade de-excitations via the 2<sup>+</sup> first excited state. Additional gamma-gamma coincidence spectra, taken with transitions from higher excited states, were not useful since they only revealed the 334-keV transition with significant intensity. Although they also indicated some very low intensity lines from extremely weakly populated higher levels, no consistent assignment could be made for these levels. The 712- and 736-keV gamma rays were not resolved in the NaI spectra, but again were resolved with the Ge(Li) detector and the internal-conversion-electron spectrometer.

The transitions mentioned above are all present in the spectrum taken in coincidence with backscattered ions. In this spectrum the region around 773 keV is obscured by a sum peak of (334+439) keV, while sum coincidences of 334 keV with 712- and 736-keV gamma rays appear at 1046 and 1071 keV. An additional transition also appears at an energy of 1193 keV. Since the latter is not evident in any of the gamma-gamma coincidence spectra, it is most probably a direct transition to the ground state. A 2<sup>+</sup> level at 1193 keV has been suggested by Smithers<sup>50</sup> but is missing in Groshev's<sup>49</sup> level scheme. Here we have identified the 859- and the 1193-keV gamma-ray as de-exciting a 2<sup>+</sup> level at 1193 keV, in agreement with Smithers' measurements. The other gamma rays mentioned have been assigned as shown in the level scheme in Fig. 12. Excitations of the 1166- and

1279-keV levels, reported previously, are either absent or very weak, which may suggest that they are not collective in character. The magnitude of the octupole reduced transition probabilities found for the excitation of 3<sup>-</sup> levels are consistent with the values found for the collective octupole states in Sm<sup>154</sup> and Sm<sup>152</sup>.

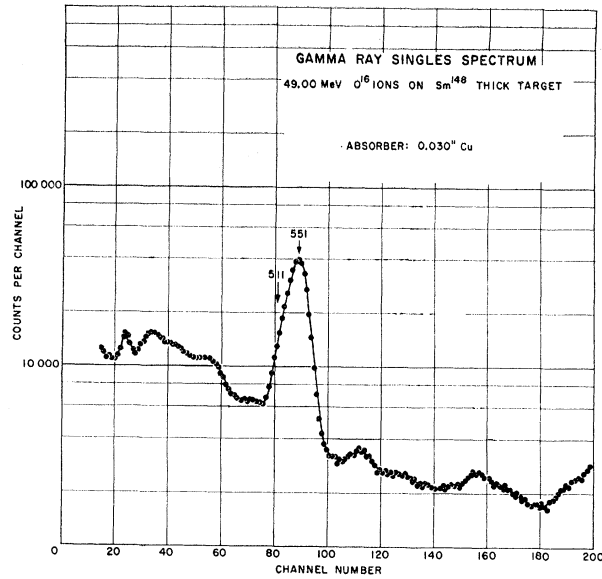
#### D. Samarium 148

As is expected when moving from the rotational toward the vibrational region in these transition nuclei, in Sm<sup>148</sup> the first few excited states lie generally higher than in the other three nuclei already discussed. For this reason only a few of the lowest collective levels were populated in this experiment. The levels of Sm<sup>148</sup> have been investigated in radioactive decay work and through (*dp*) and (*pp'*)<sup>52</sup> reaction studies. Coulomb excitation of the 551(2<sup>+</sup>)-keV first excited state has been previously observed.<sup>54</sup> Hansen and Nathan<sup>37</sup> have also reported the excitation of a state at 1165 keV which they have identified as a (3<sup>-</sup>) octupole vibration. Four excited states were observed in the present work which corroborate the previously reported energy level structure.

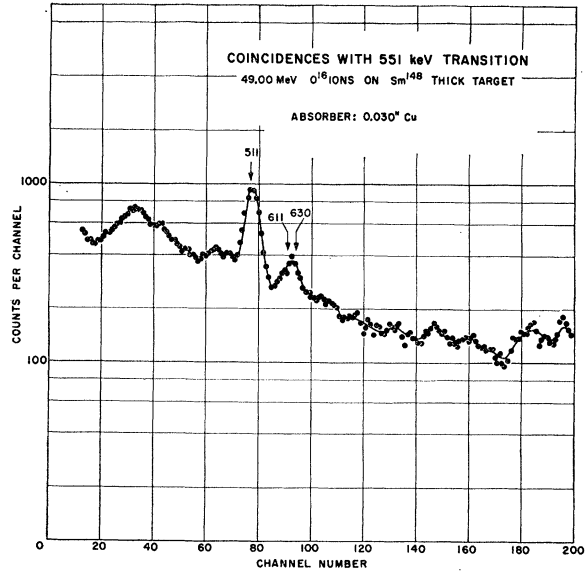
The direct gamma-ray spectrum from Sm<sup>148</sup> [Fig. 14(a)] shows only one strong transition at 551 keV. There are also lines at 435, 705, and at approximately 1020 keV, but these are of low intensity and can be attributed to expected transitions in target surface contaminants. Coincidences taken with the 551-keV transition from the first excited state [Fig. 14(b)] show a definite broad peak centered at about 620 keV and a series of very weak transitions above that energy. Using the data obtained from the radioactive decay studies, this peak has been decomposed into two lines at 611 and 630 keV which originate from 3<sup>-</sup> and 4<sup>+</sup> levels, respectively. In the gamma-particle coincidence spectrum [Fig. 14(c)], the 4<sup>+</sup> → 2<sup>+</sup> de-excitation appears as a shoulder on the 551-keV peak. The 914-keV transition seen in the latter spectrum has been identified as the 1<sup>-</sup> → 2<sup>+</sup> transition from a level at 1465 keV.

No evidence was found for the 0<sup>+</sup> and 2<sup>+</sup> members of the two-phonon triplet expected in a vibrational model at about the same energy as the 4<sup>+</sup> level. However, if their excitation energy was close to that of the 4<sup>+</sup> state, they would not have been resolved. In addition, the 0<sup>+</sup> and 2<sup>+</sup> states are expected to be less strongly excited by Coulomb excitation than the 4<sup>+</sup> state which was only weakly populated in these studies and therefore they may have gone undetected. There are indications of a broad, low-intensity, peak at approximately 1220 keV in the gamma-particle coincidence spectrum. Because of its very low intensity it did not appear in the gamma-gamma coincidence spectrum and therefore was not assigned in the level scheme shown in Fig. 15.

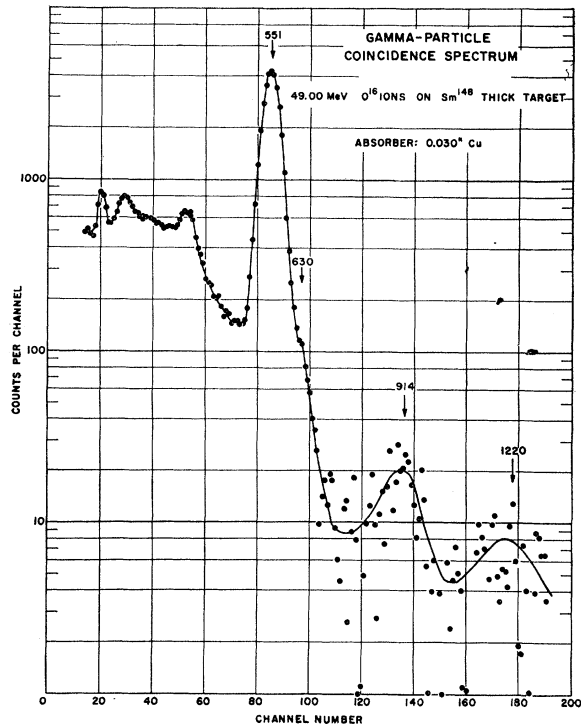
<sup>54</sup> N. P. Heydenberg and G. M. Temmer, Phys. Rev. **100**, 150 (1955).



(a)



(b)



(c)

FIG. 14. Gamma-ray spectra obtained from 49-MeV  $O^{16}$  ions on  $Sm^{148}$ : (a) direct singles spectrum; (b) spectrum taken in coincidence with the 551 keV ( $2^+ \rightarrow 0^+$ ) transition; (c) particle-gamma coincidence spectrum.

V. TRANSITION RATES

Absolute transition rates were obtained from the spectra already described by integrating the gamma-ray yields under the photopeaks and correcting these for known backgrounds, cascading decays, geometry factors, photopeak efficiencies, absorber effects, multi-channel-analyzer losses, and internal-conversion com-

petition. (For the latter the internal-conversion coefficients of Sliv and Band<sup>55</sup> have been used.) In the gamma-particle coincidence experiments, the effective particle-detector solid angle was calculated and corrected for center-of-mass motion; the energy cutoff for

<sup>55</sup> L. A. Sliv and I. M. Band, Report No. 57 ICC, Physics Department, University of Illinois (unpublished).

thick-target integrations was determined as described in Sec. III. In the gamma-gamma coincidence experiments a correction was made for the finite width of the electronic gates in determining the efficiency of the gating counter. The efficiency of the gamma-ray counters was calculated as described in Sec. III, where the estimated error with which this efficiency is known is also presented. The error quoted with the measured gamma-ray intensities in Tables I and II includes the uncertainties in all the above considerations, the statistical error, and uncertainties in determining the backgrounds and peaks in the complex spectra.

The gamma-ray yields have also been corrected for the effects of angular correlations. These corrections are approximate because of the existing ambiguities regarding the details of the excitation mechanism, and the approximations involved in evaluating the excitation amplitudes. In general because of the particular geometries used, the effects were found not to be large and the error in evaluating them was estimated as being, in most cases, small compared to the other errors quoted above.

If the gamma-ray detector is not polarization-sensitive, and if scattered ions are detected symmetrically about the beam direction, then the angular correlation appropriate to the gamma-particle measurements may be written as

$$W(\theta_\gamma) = \sum_{\text{even } k} a_k A_k (J_k/J_0) P_k(\cos\theta_\gamma),$$

where  $\theta_\gamma$  is measured relative to the beam direction,  $A_k$  is the normal gamma-gamma angular correlation coefficient,  $a_k$  is the particle coefficient, and  $(J_k/J_0)$  is an attenuation coefficient reflecting the finite solid angle subtended by the counter. The evaluation of the coefficient  $a_k$  requires assumption of the excitation mechanism, and for thick targets an integration over the relevant energy interval must be performed. For  $E2$  transitions only two terms can be involved in the expansion.

The gamma rays in the gamma-particle coincidence

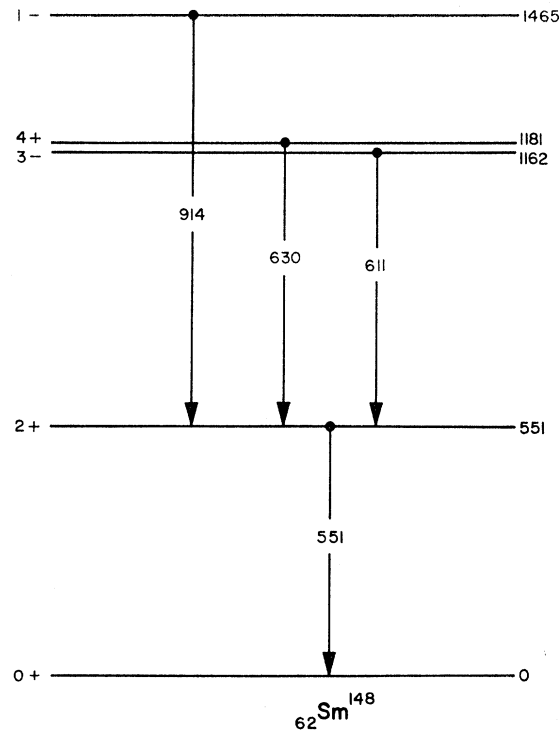


FIG. 15. Level scheme for  $\text{Sm}^{148}$ .

experiments were measured at  $55^\circ$  to the beam direction where  $P_2[\cos(55^\circ)] = 0$ . The correlation then arises only from the  $P_4$  term and is further attenuated by  $(J_4/J_0)$ .

In the gamma-gamma coincidence experiments a triple correlation is involved between the beam direction and the directions of the two gamma rays. These correlations were calculated from that of three gamma rays in cascade by multiplying the factor for the first gamma ray by  $a_k$  before summing over the three quantum numbers. Tables of Sharp *et al.*<sup>56</sup> and of Rose and Biedenharn<sup>57</sup> were used to calculate the correlation coefficients.

TABLE I. Comparison of ground-state band-transition probabilities with multiple-Coulomb-excitation-theory calculations (Refs. 32, 33, 34). All yields are normalized to one microcoulomb of integrated beam current.  $R_1$ ,  $R_2$ , and  $R_3$  refer to comparisons with the calculations using the first-order correction in  $\xi$  by Alder and Winther (Ref. 32), the diagonalization method by Alder (Ref. 33), and Berson (Ref. 34), and the latter with the yield for the state with spin  $I$  calculated with a value for  $\xi$  deduced from the energy-level spacing between the state with spin  $I$  and the state with spin  $(I-2)$ . It has been assumed that  $B(E2, 0^+ \rightarrow 2^+) = 3.40e^2 \times (10^{-48} \text{ cm}^4)$  for  $\text{Sm}^{152}$ , and  $4.61e^2 \times (10^{-48} \text{ cm}^4)$  for  $\text{Sm}^{154}$ .

	$I$	$E$ (keV)	$\xi$	Expt. yield	Theor. yield 1	$R_1$ (expt./theor.)	Theor. yield 2	$R_2$ (expt./theor.)	Theor. yield 3	$R_3$ (expt./theor.)
$\text{Sm}^{152}$	2	122	0.062	3.06 ± 0.71	2.71 ± 0.19	1.13 ± 0.27	2.71 ± 0.19	1.13 ± 0.27	...	...
	4	245		0.353 ± 0.41	0.385 ± 0.024	0.92 ± 0.13	0.334 ± 0.021	1.06 ± 0.15	0.352 ± 0.022	1.00 ± 0.14
	6	340		0.0183 ± 0.0026	0.0291 ± 0.0020	0.63 ± 0.10	0.0144 ± 0.0010	1.27 ± 0.20	0.0174 ± 0.0012	1.05 ± 0.17
$\text{Sm}^{154}$	2	82	0.041	3.11 ± 0.40	3.06 ± 0.16	1.02 ± 0.14	3.11 ± 0.23	1.00 ± 0.15	...	...
	4	185		0.594 ± 0.77	0.712 ± 0.046	0.84 ± 0.11	0.652 ± 0.0044	0.91 ± 0.12	0.657 ± 0.045	0.90 ± 0.14
	6	278		0.0389 ± 0.0054	0.0657 ± 0.0037	0.59 ± 0.07	0.0438 ± 0.0025	0.89 ± 0.11	0.0454 ± 0.0026	0.86 ± 0.14
	8	360		0.00151 ± 0.00034	0.00344 ± 0.00015	0.44 ± 0.10	0.00156 ± 0.00006	0.97 ± 0.22	0.00175 ± 0.00007	0.86 ± 0.20

<sup>56</sup> R. D. Sharp, J. M. Kennedy, M. G. Sears, and B. Hoyle, Chalk River Report No. CRT-556 (unpublished).

<sup>57</sup> L. C. Biedenharn and M. E. Rose, Rev. Mod. Phys. 25, 729 (1953).

TABLE II. Summary of results on the transition matrix elements for nonrotational states in the four even Sm isotopes. M.C.E. denotes multiple Coulomb excitation;  $\sigma_T$  denotes direct singles gamma-ray measurement;  $d\sigma/d\Omega$  denotes gamma-particle coincidence measurement.

Isotope	Transition	Excitation mode $E\lambda$	Method	$\uparrow B(E\lambda)$ $e^2(10^{-24} \text{ cm}^2)^\lambda$	$\uparrow B(E2)_{\text{corrected}}$ $e^2 \times (10^{-48} \text{ cm}^4)$
Sm <sup>154</sup>	$0^+ \rightarrow 3^-$ 1012 keV	$E3$	$\sigma_T$	$> (11 \pm 3)$	
Sm <sup>152</sup>	$0^+ \rightarrow 2_{\beta}^+$ 811 keV	M.C.E.	$d\sigma/d\Omega$	$0.068 \pm 0.015$	$0.070 \pm 0.016$
	$0^+ \rightarrow 2_{\gamma}^+$ 1087 keV	M.C.E.	$\sigma_T$	$0.109 \pm 0.020$	$0.119 \pm 0.024$
Sm <sup>150</sup>	$0^+ \rightarrow 2^+$ 334 keV	$E2$	$\sigma_T$	$1.25 \pm 0.21$	
		M.C.E.	$\sigma_T$	$1.31 \pm 0.21$	
	$2^+ \rightarrow 0^+$ 407 keV	$E2-E2$	$\sigma_T$	$0.041 \pm 0.020$	
	$2^+ \rightarrow 4^+$ 439 keV	$E2-E2$	$\sigma_T$	$0.95 \pm 0.20$	
	$2^+ \rightarrow 2'^+$ 712 keV	$E2-E2$	$\sigma_T$	$0.39 \pm 0.12$	
	$0^+ \rightarrow 3^-$ 1070 keV	$E3$	$\sigma_T$	$0.36 \pm 0.10$	
	$0^+ \rightarrow 3^-$ 1358 keV	$E3$	$\sigma_T$	$0.15 \pm 0.04$	
	$2^+ \rightarrow 2''^+$ 859 keV	$E2-E2$	$\sigma_T$	$0.042 \pm 0.021$	
	$0^+ \rightarrow 2''^+$ 1193 keV	$E2-E2$	$\sigma_T$	$0.089 \pm 0.044$	
Sm <sup>148</sup>	$0^+ \rightarrow 2^+$ 551 keV	$E2$	$\sigma_T$	$0.89 \pm 0.10^a$	
	$2^+ \rightarrow 4^+$ 630 keV	$E2-E2$	$\sigma_T$	$0.62 \pm 0.33$	
	$0^+ \rightarrow 3^-$ 1162 keV	$E3$	$\sigma_T$	$0.23 \pm 0.13$	

\* Data from B. Elbek *et al.*, Nucl. Phys. 19, 523 (1960).

In the calculation of reduced transition probabilities, from the experimental yields, the error in the ionization energy loss for the thick-target integrations is estimated to be  $\pm 5\%$  based on a comparison of the semiempirical range curves with range measurements for oxygen in nickel and on the validity of the customary linear extrapolation with the atomic number  $Z$  of the material [Eq. (2)]. Interpolation errors in the Coulomb excitation theory are estimated to be about  $0.5\%$  for direct excitation calculations,  $1\%$  for multiple Coulomb excitation, and  $2\%$  for double excitations. This obviously assumes that a correct theory is being used and that the excitation mechanism is understood. Additional uncertainties reflect those in the parameters used in the theory. These have been included in the errors quoted for the reduced transition probabilities.

In the following subsections we shall extract these matrix elements from the available data for both rotational and nonrotational excitations in the samarium nuclei under study.

### A. Ground-State Rotational-Band Excitations

For heavy ions with sufficiently high bombarding energies, the excitation cross section between members of a rotational band in a strongly deformed nucleus with a large quadrupole moment becomes comparable to unity so that the perturbation treatment of the excitation mechanism becomes invalid. In such cases the interaction between the exciting particle and the nucleus is of sufficient strength so that many levels are strongly involved in the excitation processes. Using the semiclassical approximation, Alder and Winther<sup>32</sup> have calculated the excitation amplitudes in this strongly coupled situation in the impact approximation ( $\xi=0$ , where  $\xi$  is the usual adiabatic parameter), neglecting the energy differences between levels for  $180^\circ$  scattering of the bombarding particle. Scattering at other angles was

computed in the so-called  $\chi(\theta)$  approximation.<sup>32</sup> For backscattering angles this approximation is expected to yield fairly accurate results in the impact approximation.

In all these calculations the model of an axially symmetric nucleus is assumed with pure rotational wave functions. The effects of mixing with higher lying vibrational or intrinsic states have been neglected. These effects are expected to be small since they are reduced by the ratio of the interband to intraband transition moments.

Corrections for finite  $\xi$  have been evaluated by Alder and Winther<sup>32</sup> to first order and more directly by Alder<sup>33</sup> and Berson<sup>34</sup> using a matrix diagonalizing procedure in which five rotational states are included. Comparisons with both calculations are made below. The effects of considering a finite number of levels on the excitation of the higher spin states is discussed by Berson,<sup>34</sup> who shows that the excitation of the  $I^\pi=6^+$  state will be negligibly affected by cutting off the diagonalization procedure at five states. In general, increasing  $\xi$  depresses the excitation cross section for high spin states relative to those for  $\xi=0$  and moves the peak of the predicted differential cross section to forward angles. For  $\xi \neq 0$ , the  $\chi(\theta)$  approximation introduces some small presently unknown error.

The Coulomb excitation amplitudes for the levels of a pure rotator may be parameterized by two quantities, the adiabaticity parameter  $\xi$ , and a quantity  $q$  defined below.  $\xi$  is related to the moment of inertia  $\mathcal{I}$  by

$$\xi = Z_1 Z_2 A_1^{1/2} \Delta E' / 12.65 (E - \frac{1}{2} \Delta E')^{3/2}, \quad (3)$$

where  $\Delta E' = (3\hbar^2/\mathcal{I})(1 + (A_1/A_2))$  for the transition ( $I=0 \rightarrow I=2$ ). All energies are in MeV, and the subscripts 1 and 2 refer to the bombarding ion and target nucleus, respectively. The parameter  $q$  is related to the

intrinsic quadrupole moment  $Q_0$ , by

$$q = 7.624A_1^{1/2}Q_0E^{3/2}Z_1^{-1}Z_2^{-2}(1 + (A_1/A_2))^{-2}. \quad (4)$$

$Q_0$  is measured in units of ( $10^{-24}$  cm<sup>2</sup>). For the pure rotational model,  $Q_0$  for the band and the individual reduced transition probabilities between members of the band of an even-even nucleus are fixed by

$$B(E2, I \rightarrow I+2) = \frac{15}{32\pi} \frac{1}{e^2 Q_0^2} \frac{(I+1)(I+2)}{(2I+1)(2I+3)}. \quad (5)$$

Deviations from Eq. (5), and the variation of the moment of inertia with spin are obviously not considered in this formulation.

Table I compares the experimental and calculated thick-target yields for Sm<sup>154</sup> and Sm<sup>152</sup> in the particle-coincidence experiments. The theoretically expected yields were obtained using the Alder-Winther<sup>32</sup> calculations with first-order corrections for finite  $\xi$ , the matrix-diagonalization procedure mentioned above,<sup>34,35</sup> and, finally, the latter with the yield for the state with spin  $I$  calculated with a value for  $\xi$  deduced from the energy-level spacing between the state with spin  $I$  and the state with spin  $(I-2)$ . The  $B(E2, I=0 \rightarrow I=2)$  values were obtained from the inelastic proton-scattering data of Elbek *et al.*<sup>58</sup> The errors indicated with the calculated yields result from uncertainties in interpolation,  $dE/dS$  determination, target-thickness cutoff, beam energy, and the angle subtended by the particle counters. All yields have been normalized to an arbitrarily chosen unit of beam integration.  $\xi$  was calculated using Eq. (3). Column 4 lists the experimental yields, columns 5, 7, and 9, respectively, show the yields calculated under the three conditions mentioned above. The ratios of the experimental-to-calculated yields ( $R_i$ ) are listed in columns 6, 8, and 10.

It is evident that the best agreement between the experimental and calculated thick-target yields is obtained for the case in which the matrix diagonalization procedure is employed for the latter. The mean values for  $R_2$  tend to be systematically high for Sm<sup>152</sup>, and low for Sm<sup>154</sup>, although they are close to unity within the quoted errors. It may be noted that a small change in the  $B(E2, I=0 \rightarrow I=2)$  values used can remove the discrepancy between the mean values of the calculated and experimental yields. The higher spin states are particularly sensitive to this parameter. However, because of the existing uncertainties in the analysis of the experimental normalization error, and the approximate nature of excitation theory used, these measurements cannot presently be considered as an independent check on the value for the  $B(E2, I=0 \rightarrow I=2)$  obtained from the inelastic-scattering measurements.<sup>58</sup>

The analysis leading to the ratio  $R_2$  did not take into account the possible variation of the moment of inertia

and of the  $B(E2)$  with spin. These effects are expected to be important for the higher spin states in Sm<sup>152</sup> where deviations from the  $I(I+1)$  rotor energy-interval rule are very apparent.

The effect of a variation in the moment of inertia, and therefore in  $\xi$ , may be estimated by assuming a  $\xi$  for the calculated excitation of the spin- $I$  level corresponding to a moment of inertia derived from the energy-level spacing between the spin- $I$  and  $(I-2)$  states instead of that between the  $0^+$  and  $2^+$  states. This approach leads to an overestimate of the magnitude of this effect. The resulting modifications in the calculated yields and in  $R_2$  are tabulated in columns 9 and 10 in Table I. It is evident that the inclusion of centrifugal stretching would improve the agreement with experiment for the higher spin states in Sm<sup>152</sup>.

The effect of a variation in the  $B(E2)$  with spin cannot be treated in the context of the presently available multiple-excitation theory; but again, it is expected that for a soft rotor like Sm<sup>152</sup> it may be important to include this effect in an accurate description of the excitation of states with large spin.

## B. Nonrotational Excitations

The Coulomb excitation of states which differ from the ground state in their intrinsic structure (here we also include vibrational excitations) was analyzed using two approaches. For reasons discussed below, in the nearly spherical nuclei, first- and second-order perturbation theory was used, and in cases involving rotational states in the excitation process, multiple-Coulomb-excitation theory was employed.

The probability of exciting states in Sm<sup>148</sup> and Sm<sup>150</sup> is sufficiently small at the bombarding energies used in these measurements to expect that the total cross section for a thick target (integrated over the scattered-particle direction) will be accurately approximated by a first- and second-order perturbation calculation.<sup>33,36</sup> Studies of the excitation of states in another mass region (with characteristics similar to those populated in the above two nuclei), by Stelson and McGowan<sup>59</sup> using  $\alpha$  particles, and by Eccleshall *et al.*,<sup>60</sup> using O<sup>16</sup> ions, substantiate this view. As a guide to the accuracy to be expected, it may be noted that a first-order perturbation calculation of the excitation probability for the first  $2^+$  state of Sm<sup>150</sup>, at 334 keV, differs by only 5% from that obtained in an analysis using the multiple-Coulomb-excitation theory for a pure vibrational model derived by Alder and Winther<sup>32</sup> and also by Robinson.<sup>61</sup> The difference arises from depopulation of the first excited state by higher order transitions to the higher lying collective states which are neglected in the first-order

<sup>59</sup> P. H. Stelson and F. K. McGowan, Phys. Rev. **121**, 499 (1961).

<sup>60</sup> D. Eccleshall *et al.*, Nucl. Phys. **37**, 377 (1962).

<sup>61</sup> D. W. Robinson, Nucl. Phys. **25**, 459 (1961).

<sup>58</sup> B. Elbek, M. C. Olesen, and O. Skilbreid, Nucl. Phys. **19**, 523 (1960).

theory. In second order, reorientation effects may also contribute, although these are neglected here.<sup>62</sup>

Somewhat more caution must be exercised in dealing with the differential cross section when the inelastically scattered ions are detected near the backward direction in coincidence with gamma radiations. In this case, the probability of excitation becomes fairly large for the conditions of this experiment, and therefore larger errors can be intuitively anticipated when perturbation theory is used. However, again comparisons made with the model-dependent multiple-Coulomb-excitation calculations<sup>36</sup> indicate that these errors are small for most states under consideration below. It may be noted that the measurements by Eccleshall *et al.*<sup>60</sup> on thick targets also show that the errors are not large.

Using the above considerations as a guide, the excitation of the  $0^+$ ,  $2^+$ ,  $2'^+$ ,  $2''^+$ ,  $4^+$ , and  $3^-$  states in  $\text{Sm}^{148}$  and in  $\text{Sm}^{150}$  were analyzed using first- and second-order perturbation theory. This approach, of course, is model-independent, and therefore in principle allows the extraction of the reduced transition probabilities in a model-independent way. For  $4^+$  and  $0^+$  states, double  $E2$  excitation has been used, and for  $3^-$  states a direct  $E3$  excitation. The second and higher  $2^+$  states can be populated in lowest first and second order by either a direct  $E2$  excitation from the ground state or a double  $E2$  excitation by way of the first  $2^+$  state. In general, these two amplitudes are coherent with an unknown relative phase between the matrix elements  $\langle 0||E_2||2' \rangle$  and the product of  $\langle 0||E_2||2 \rangle$  and  $\langle 2||E_2||2' \rangle$  so that when the amplitude  $\langle 0||E_2||2' \rangle$  is not ruled out by experiment as a negligible contribution, the  $B(E2, 2 \rightarrow 2')$  or  $B(E2, 0 \rightarrow 2')$  extracted from our experimental transition probabilities are double-valued. In principle the relative sign of these matrix elements can be determined from the behavior of the cross section with bombarding energy. There were not sufficient data available in the present experiments to make a unique assignment. For all the nuclei being considered, the  $2 \rightarrow 2'$  transition is always present with a significant intensity. In the framework of the pure vibrational model it would be expected that the crossover transition  $0 \rightarrow 2'$  would be either absent or weak. The multipolarity of the  $2' \rightarrow 2$  transition has been assumed to be pure  $E2$  in determining the ratio  $\Gamma(E2, 2' \rightarrow 2)/\Gamma(E2, 2' \rightarrow 0)$  from the experimental branching ratio of the decay of the  $2'$  state. From previous work this is expected to be a fairly good assumption for the states that exhibit a collective, near-harmonic behavior.

All the double-excitation calculations were performed using the numerical formulas and tables made available by Douglas<sup>63</sup>; the multiple-Coulomb-excitation calculations, based on the pure vibrational model, followed those of Alder and Winther<sup>32</sup> and of Robinson.<sup>61</sup>

For the deformed nuclei,  $\text{Sm}^{154}$  and  $\text{Sm}^{152}$ , the above approach must be modified since the excitation process may become considerably more complex through participation of levels both in the ground-state rotational band and in the rotational band based on intrinsic states. Although it may be a good approximation to describe the transitions between intrinsic states with first-order perturbation theory, the high probability of virtual transitions in the ground-state band before the intrinsic excitation, and similar virtual transitions between members of the upper band after the transitions between the intrinsic states, must strongly influence the mechanism of excitation. In addition, band mixing may seriously affect the transition probability between intrinsic states, since the Coulomb excitation amplitude from the admixture is proportional to large transition moments between identical intrinsic states. The latter is of considerable importance in determining the transition moments to the beta and gamma vibrational bands in  $\text{Sm}^{152}$  in the limit of vanishing interband mixing, as we shall indicate below.

The excitation of the vibrational bands in  $\text{Sm}^{154}$  and  $\text{Sm}^{152}$  were analyzed using calculations by Alder,<sup>33</sup> and by Lutken and Winther.<sup>36</sup> In the latter, again as in the ground-state rotational-band calculations, the excitation amplitudes are considered within the framework of the Bohr-Mottelson model, and the populations of rotational band members based on vibrational modes of excitation are evaluated by treating the transitions between bands with first-order perturbation theory, and the virtual transitions within a rotational band as multiple-Coulomb excitations in the impact approximation. For the even-even nuclei being considered, the resulting excitation probability for a state of spin  $I$  and spin projection  $K$  along the symmetry axis factors into a product of two terms, the first-order perturbation probability  $[\chi^\lambda(\theta\xi)]^2$  for the direct excitation to the band and a redistribution function  $|B_{IK}^{\lambda\mu}(q)|^2$  which describes the sharing of the total transition strength to the band among the band members. Normalization requires that  $\sum_I |B_{IK}^{\lambda\mu}(q)|^2 = 1$ ;  $\lambda$  refers to the multipolarity of the transition. This implies that the total excitation probability of the upper band is that given by the ordinary perturbation treatment, and the effect of the multiple excitation, internal to the band, is a redistribution of the total probability among the band members. This result can be used to extract the reduced transition strength between the ground-state band and the excited band by considering either the total measured intensity to the band, or the individual level populations.

As mentioned above, the calculations employ the impact approximation ( $\xi=0$ ) for transitions between states belonging to the same rotational band. This assumption does not introduce an appreciable error in the calculations of the excitation probabilities for the gamma-particle coincidence experiments where  $\xi < 0.06$ . The effects of a small, finite  $\xi$  may be examined quali-

<sup>62</sup> G. Breit, R. L. Gluckstern, and J. E. Russell, Phys. Rev. **103**, 727 (1956); **105**, 1121 (1957).

<sup>63</sup> A. C. Douglas, Nucl. Phys. **42**, 428 (1963); Atomic Weapons Research Establishment Report No. NR/P-2/62 (unpublished).



tatively by referring to Table I and data obtained elsewhere<sup>35</sup>; this indicates that small departure from  $\xi=0$  will only have a significant effect on higher order excitations than the first. Here we are only concerned with a redistribution of the total transition strength to the upper band by not more than two transitions within the band, and usually only a single one. It may be pointed out that for the above reason the lower average energies involved in the total excitation-cross-section measurements on a thick target make such measurements less reliable for the extraction of transition moments from the individual population of states in the vibrational bands.

A further approximation has been made below in evaluating the redistribution function,  $B_{IK^{\lambda\mu}}(q)$  for the natural parity states,  $(I+\lambda)$  even. Following the treatment of the ground-state band, the dependence of the total excitation probability on the scattering angle has been calculated in the  $q(\theta)$  approximation,<sup>32</sup> where one considers the  $\mu=0$  magnetic substate amplitude to dominate and the  $\mu \neq 0$  terms to be negligible. This approximation is expected to be most reliable for  $\theta$  approaching  $180^\circ$ . Comparisons with calculations<sup>36</sup> in which all magnetic substates are considered show that for the natural parity states in the octupole, gamma, and beta vibrational bands, the error introduced with the  $q(\theta)$  approximation is small compared with the other present uncertainties in the measurements. The unnatural parity states,  $(I+\lambda)$  odd, have to be dealt with separately since in the  $q(\theta)$  approximation they are not excited.

The numerical formulas used for computing the excitation probability of the natural parity states are as follows,<sup>36</sup> for pure multipole transitions:

$$P_{I_f, K_f} = [\chi^\lambda(\theta, \xi)]^2 (2I_f + 1) \times \sum_I \begin{pmatrix} I_f & I_i & I \\ -K_f & K_0 & K \end{pmatrix} |B_{IK^{\lambda 0}}(q(\theta))|^2, \quad (6)$$

with

$$\chi^\lambda(\theta, \xi) = \chi^\lambda \left( \sum_{\mu} [R_{\lambda\mu}(\theta, \xi)]^2 \right)^{1/2}. \quad (7)$$

The notation is standard.<sup>36</sup> The multipolarities considered have been quadrupole,  $\lambda=2$ , and octupole,  $\lambda=3$ .  $R_{\lambda\mu}(\theta, \xi)$  are functions of the orbital integrals tabulated by Lutken and Winther;<sup>36</sup>  $q(\theta) = qR_{20}(\theta, 0)$ ;  $q$  has been defined in Eq. (4);  $\chi^\lambda$  is the first-order perturbation theory excitation probability (for  $\theta=\pi$  and  $\xi=0$ ) for the directly attainable member of the upper band;  $B_{IK^{\lambda 0}}(q)$  are the redistribution probabilities tabulated by Lutken and Winther,<sup>36</sup> and related to the ordinary multiple-Coulomb-excitation-theory amplitudes. For lack of any more specific information the intrinsic quadrupole moments for the upper bands have been assumed to be the same as that for the ground-state band in all computations. This assumption is not necessarily valid even for a pure rotational model. For unnatural parity states the

summation over the magnetic quantum number  $\mu$  has to include also  $B_{IK^{\lambda\mu}}(q)$ .

In arriving at the predicted probabilities the appropriate integration was performed over the thick target and scattering angles. Figures 8 and 10 show the differential cross sections for the individual states in the beta and octupole bands for the bombarding conditions encountered in this particular experiment; an average  $\xi$  and  $q$  were used. The typical behavior with spin, and its usefulness in identifying levels, have been discussed previously in Sec. IV. No band-mixing effects have been included in the computations leading to Figs. 8 and 10.

The band-mixing effects have been considered by Lutken and Winther<sup>36</sup> in a first-order perturbation treatment in which the mixing is expressed through the modification of the multipole operators while maintaining pure rotational wave functions. An equivalent description is discussed herein in which the coupling between rotational and intrinsic motion admixes the pure rotational and vibrational bands and therefore modifies the interband de-excitation transition probabilities. The effects of interband mixing on Coulomb excitation and de-excitation probabilities of course are similar. The Lutken and Winther approach, however, shows in a transparent way that the effect on the Coulomb-excitation amplitude arises from a change in the intrinsic matrix element of the quadrupole moment which results generally in a renormalization of  $\chi$ .

The calculations have been carried out in an approximate manner, using the  $\mu=0$  approximation which is least applicable in determining the population of these states for which the band-mixing corrections turn out to be large, i.e., for final-state spins of 2 or 4. There is therefore considerable uncertainty associated with using the observed excitation of these states in evaluating the interband transition matrix elements in the limit of zero mixing. For the beta band in  $\text{Sm}^{152}$ , which is of primary interest here, the  $0^+$  state population obtained from the observed differential cross section leads to the most accurate value for the reduced interband matrix element; in this case only small mixing corrections have to be applied, the various approximations in the excitation theory are best satisfied, and the experimental yield has been obtained with good accuracy.

The results of measurements on the excitation of intrinsic states for the four samarium isotopes investigated are summarized in Table II. All measurements listed were performed at a beam energy of 49 MeV. Column 1 lists the isotope; column 2 lists the transition for which the  $\uparrow B(E\lambda)$  is being determined, with the energy of the transition given in parentheses; column 3 gives the mode of excitation assumed in calculating the excitation probability to the final state. Column 4 specifies the measurement performed, with  $\sigma_T$  referring to a total-cross-section measurement from both direct and gamma-gamma coincidence spectra, and  $d\sigma/d\Omega$  referring to a gamma-particle coincidence measurement;

TABLE III.  $B(E3)$  values for collective octupole states in Sm isotopes 148, 150, 152, and 154.

Isotope	$E_{3^-}$ (keV)	$\uparrow B(E3)$ (in S.P. units) <sup>a</sup>
Sm <sup>148</sup>	1162	25±14
Sm <sup>150</sup>	1070	38±11
	1358	15±5
Sm <sup>152</sup>	1045	15±5
Sm <sup>154</sup>	1012	> (11±3)

<sup>a</sup> S.P. denotes single-particle units as defined in text.

$\uparrow B(E\lambda)$ , in units of  $e^2(10^{-24} \text{ cm}^2)^\lambda$ , as determined from the measurements, is given in column 5; column 6 is the  $\uparrow B(E2)$  value in units of  $e^2(10^{-48} \text{ cm}^4)$  after a correction has been applied for interband mixing in the cases where the mixing coefficient has been determined.

### 1. Odd-Parity States

In Sm<sup>154</sup> three members of an octupole band for which a specific identification could be made were excited. The  $\uparrow B(E3)$  value for the  $3^-$  state was obtained from the measured total excitation to the band using the Lutken-Winther description of the excitation mechanism. Since only the 636-, 745-, and 914-keV transitions could be measured with reasonable accuracy, a lower limit for  $B(E3, 0^+ \rightarrow 3^-)$  was determined to be  $(11 \pm 3)e^2 \times (10^{-74} \text{ cm}^6)$ . This is in good agreement with the value of  $(15 \pm 6)e^2 \times (10^{-74} \text{ cm}^6)$  reported by Hansen and Nathan.<sup>37</sup> The individual population of the members of the band could not be determined since several gamma transitions were undetected. In the case of the  $5^-$  state, where a branching ratio is available, it was found that  $B(E1, 5^- \rightarrow 6^+)/B(E1, 5^- \rightarrow 4^+) = 0.86 \pm 0.32$ , which can be compared with the pure  $K=0$  band de-excitation branching ratio of 1.20 predicted by Alaga.<sup>44</sup>

As pointed out in Sec. IV, enhanced octupole transitions to the low-lying  $3^-$  states were also found in the other three Sm nuclei; the  $B(E3)$  values from 10 to approximately 35 single-particle units indicate the collective nature of these states. These data are summarized in Table III. We define the single-particle unit used in this work by

$$\uparrow B(E\lambda)_{\text{s.p.}} = (2\lambda + 1)e^2/4\pi(3/3 + \lambda)^2 R_0^{2\lambda}. \quad (8)$$

The accuracy with which the  $\uparrow B(E3)$  value is known in Sm<sup>148</sup> is poor, ( $\pm 50\%$ ) reflecting the close proximity in energy of a 630-keV transition ( $4^+ \rightarrow 2^+$ ). Two  $3^-$  levels were excited in Sm<sup>150</sup>. The intensities for the 585-keV and 1024-keV de-excitation transitions were combined to determine the population of the 1358-keV state. The 1024-keV gamma ray has not been definitely assigned to the 1358-keV level by either Groshev<sup>49</sup> or Smithers.<sup>50</sup> It appears quite clearly in the gamma-ray spectrum taken in coincidence with the 334-keV transition.

### 2. Even-Parity States of Sm<sup>148</sup> and Sm<sup>150</sup>

The predictions of the simple phonon model of quadrupole vibrations and of the simple asymmetric rotor model for  $\gamma = 21.6^\circ$  as obtained from the  $E(2^+)/E(2^+)$  ratio are compared in Table IV with the  $\uparrow B(E2)$  values measured for transitions between the even-parity states in Sm<sup>150</sup>. In obtaining the latter ratio the  $2^{'+}$  state is assumed to be at an excitation of 1046 keV. A comparison with the simple phonon model is also made for Sm<sup>148</sup>.

In the calculations of double  $E2$  excitations for Sm<sup>150</sup>, a  $B(E2, 0^+ \rightarrow 2^+) = (1.32 \pm 0.06)e^2 \times (10^{-48} \text{ cm}^4)$  was taken from the inelastic-scattering data of Elbek *et al.*,<sup>58</sup> which agrees with the less precise values of  $(1.25 \pm 0.21)e^2 \times (10^{-48} \text{ cm}^4)$  obtained in this experiment assuming first-order perturbation theory, and of  $(1.31 \pm 0.21)e^2 \times (10^{-48} \text{ cm}^4)$  obtained by assuming multiple Coulomb excitation of a pure quadrupole vibrator. The difference in the latter two values arises from the term  $e^{-[\chi(\theta, E)]^2}$  which takes into account the depopulation of the lowest excited state by higher order excitations.

It is evident from Table IV that a majority of the transitions are enhanced and may be considered as collective in character. The  $B(E2, 2^+ \rightarrow 4^+)/B(E2, 0^+ \rightarrow 2^+)$  ratios predicted by the phonon model agree with experiment, but the validity of the simple asymmetric-rotor model cannot be ruled out. The value for this ratio in Sm<sup>150</sup> and Sm<sup>148</sup> follows the trend also found by Eccleshall *et al.*,<sup>60</sup> in the even-even Pd and Cd isotopes. It is also characteristic of the latter mass region that the observed  $B(E2, 2^+ \rightarrow 2^{'+})$  is usually less than that predicted by the phonon model and averages about one-half of this value. A similar situation seems to exist for the second  $2^{'+}$  level in Sm<sup>150</sup>. The third  $2^{'+}$  state behaves somewhat differently. An abnormally large crossover to cascade transition ratio is observed,  $B(E2, 0 \rightarrow 2^{'+})/B(E2, 2^+ \rightarrow 2^{'+}) \sim 2$ , whereas no ( $2^{'+} \rightarrow 0^+$ ) transitions were found either in this or in Smithers's<sup>4</sup> work. Of course, no crossover would be expected on the basis of the pure phonon model. The  $B(E2, 2^+ \rightarrow 2^{'+})$  is also much smaller than the  $B(E2, 2^+ \rightarrow 2^+)$ , and it would thus be difficult to include the  $2^{'+}$  state in a model of

TABLE IV. Comparison of  $B(E2)$  ratios in Sm<sup>150</sup> and Sm<sup>148</sup> with the simple phonon and asymmetric rotor models.

$E_\gamma$ (keV)	$I^\pi$	Experimental $B(E2, 2 \rightarrow 1)/$ $B(E2, 0 \rightarrow 2)$	Phonon model	Adiabatic asym- metric rotor model $\gamma = 21.6^\circ$
Sm <sup>150</sup>				
407	0 <sup>+</sup>	0.031±0.016	0.08	...
712	2 <sup>+</sup>	0.295±0.091	0.40	0.10
439	4 <sup>+</sup>	0.72 ±0.15	0.72	0.53
Sm <sup>148</sup>				
630	4 <sup>+</sup>	0.7 ±0.4	0.72	...

TABLE V. Mixing coefficients  $Z_\beta$  and  $Z_\gamma$  deduced from the branching ratios for the de-excitation of states in the beta and gamma bands. The notation is defined in the text.

Transition ratio ( $M$ )	Expt. ratios	$M_{\text{exp}}/M_{\text{Alaga}}$	$Z_\gamma$	$Z_\beta$
$B(E2, 2'^+0 \rightarrow 2^+0)/B(E2, 2'^+0 \rightarrow 0^+0)$	$2.36 \pm 0.70$	$1.65 \pm 0.49$		$-0.074$
$B(E2, 2'^+0 \rightarrow 4^+0)/B(E2, 2'^+0 \rightarrow 2^+0)$	$3.79 \pm 0.67$	$2.10 \pm 0.37$		$-0.064, +0.350$
$B(E2, 2'^+2 \rightarrow 2^+0)/B(E2, 2'^+2 \rightarrow 0^+0)$	$1.87 \pm 0.64$	$1.31 \pm 0.45$	$-0.045, +2.49$	
$B(E2, 3^+2 \rightarrow 4^+0)/B(E2, 3^+2 \rightarrow 2^+0)$	$0.64 \pm 0.24^a$	$1.60 \pm 0.60$	$-0.037$	

<sup>a</sup> Data from O. Nathan, Nucl. Phys. 19, 148 (1960).

collective vibrations. A state with similar properties has been reported by Stelson and McGowan<sup>59</sup> and by Eccleshall *et al.*,<sup>60</sup> in Cd<sup>114</sup>, at 1.365 MeV. In calculating  $B(E2, 2^+ \rightarrow 2'^+)$  it was assumed that  $B(E2, 0^+ \rightarrow 2'^+) = 0$  so that the interference between the double ( $E2$ ) and direct excitation amplitudes for the excitation of the  $2'^+$  state vanishes. The interference term is also negligible in the excitation of the  $2'^+$  state where the direct excitation dominates.

The first excited  $0^+$  state of Sm<sup>150</sup> appears to be collective, although this measurement is made somewhat uncertain by the nearby intense transition of 439 keV. In general, it is difficult to obtain information on the Coulomb excitation of the  $0^+$  states because of the intense competition from the usually adjacent  $4^+$  level which, in the limit of validity of the pure phonon model, is favored by a factor of  $(2I+1)$  reflecting the dependence of  $B(E2, 2^+ \rightarrow I)$  on the spin. The most favorable experimental conditions involve scattering in the backward direction in the limit as  $\xi \rightarrow 0$ . For this reason there is very little specific information available regarding transition strengths to the known  $0^+$  levels, although a number of these have been located through reaction studies other than Coulomb excitation. Such information, of course, would be very valuable in making comparisons between the existing models.

### 3. Even-Parity States of Sm<sup>152</sup>

In Sm<sup>152</sup> there is enough information available from the present measurements on vibrational levels, and rotational states based on these vibrational levels, to allow very meaningful comparisons with the existing description of collective spectra. It was pointed out in the Introduction that Sm<sup>152</sup> would represent a favorable nucleus in which to look for departures from the strong coupling, adiabatic description of rotational spectra, and that the consequences of these departures could be sensitively probed by examining the transition probability ratios for interband transitions together with the modification of the  $I(I+1)$  energy interval rule for the bands. The results for a number of transition ratios for the de-excitation of members of the beta and gamma band are summarized in Table V. Included also are measurements by Nathan<sup>64</sup> for the gamma band.

The deviations from the Alaga transition rules,<sup>44</sup> for

unmixed bands in axially symmetric nuclei, are evident from the ratios shown in column 3. The notation  $\downarrow B(E2, I_i K_i \rightarrow I_f K_f)$  is used. As was discussed in the introductory section of this paper, a possible approach toward accounting for these deviations from the adiabatic predictions is to consider, within the framework of the Bohr-Mottelson model, the admixing of the state functions in the beta, gamma, and ground-state bands brought about by differences between the exact rotational Hamiltonian and that corresponding to the adiabatic approximation. In the simplest treatment the influence of still other states are neglected as is the interaction between beta- and gamma-type vibrations themselves. The latter could be important if the beta and gamma-band head energies were nearly degenerate; a possible example may be found in Th<sup>232</sup>.<sup>13</sup>

Considering only first-order mixing, the state functions for the ground state and the lowest lying beta and gamma vibrational band members may be written as follows:

$$\psi_{n_x=1}(I_i) = \psi_{n_x=1}^K(I_i) + \epsilon_x f_x(I_i) \psi_{n_x=0}^0(I_i), \quad (9)$$

$$\psi_{n_x=0}(I_f) = \psi_{n_x=0}^0(I_f) - \epsilon_x f_x(I_f) \psi_{n_x=1}^K(I_f), \quad (10)$$

where we have written the wavefunction as  $\psi_{n_x}^K(I)$ ;  $x$  denotes  $\beta$  or  $\gamma$ , and  $n_x$  is the vibrational quantum number. The quantum numbers for the ground state, beta, and gamma-vibrational bands are, respectively  $n_\beta = n_\gamma = 0, K = 0$ ;  $n_\beta = 1, n_\gamma = 0, K = 0$ ;  $n_\beta = 0, n_\gamma = 1, K = 2$ . The admixed amplitude factor  $\epsilon_x f_x$  may be obtained from the appropriate matrix elements in the Bohr Hamiltonian<sup>8,9</sup> which mix gamma and beta bands with the ground state. These are, respectively,

$$\langle \psi_{n_\gamma=1}(I_i) | I_1^2 - I_2^2 | \psi_{n_\gamma=0}(I_f) \rangle$$

and

$$\langle \psi_{n_\beta=1}(I_i) | I_1^2 + I_2^2 | \psi_{n_\beta=0}(I_f) \rangle,$$

as discussed in earlier publications.<sup>12,23</sup> The mixing amplitude factor  $\epsilon_x f_x$  is expressed as a product of two terms of which  $f_x(I)$  contains only the angular-momentum dependence of the matrix elements;  $f_\beta(I) = I(I+1)$ , and  $f_\gamma(I) = [(I-1)I(I+1)(I+2)]^{1/2}$ . The factor  $f_x$ , as written, tacitly implies that the equilibrium deformation  $\beta_0$  is independent of the angular momentum of the state and is constant for the band. The quantities  $\epsilon_x$ , therefore also constant for a specific band, are treated here as parameters to be determined by experi-

<sup>64</sup> O. Nathan, Nucl. Phys. 19, 148 (1960).

ment; they may also be calculated by specifying the form of the moments of inertia and of the vibrational wave functions.<sup>65</sup> For the former, the analysis is model-independent except for the strong-coupling assumption, and for the angular-momentum dependence taken for the perturbing interaction which arises partly from the assumption of a predominantly axially symmetric nuclear shape. A specific model in which the hydrodynamic form for the moments of inertia have been assumed (within the framework of the Bohr-Mottelson description) has been considered by Preston and Kiang,<sup>65</sup> by Lipas,<sup>66</sup> and by Sheline.<sup>67</sup> The results of the latter calculations have not proved successful in accounting for details of the observed spectra.<sup>66,67</sup>

The reduced transition moments may be written generally as

$$B(EL, I_i K_i \rightarrow I_f K_f) = |Q(L; K_i K_f)|^2 [(I_i L K_i K | I_f K_f) - \epsilon_x \alpha_x f_x(I_f) (I_i L K_i K | I_f K_i) + \epsilon_x \alpha_x f_x(I_i) (I_i L K_f K | I_f K_f)]^2, \quad (11)$$

where

$$\alpha = Q(L; K_i K_i) [Q(L; K_i K_f)]^{-1} = Q(L; K_f K_f) [Q(L; K_i K_f)]^{-1} \quad (12)$$

is the ratio of the intrinsic multipole transition amplitude within a band to that between bands, and the customary assumption has been made that  $Q(L; K_i K_i) \simeq Q(L; K_f K_f)$ . Although small deviations from this equality may alter the final detailed answers, they will not affect appreciably the general conclusions on the success of the mechanism being discussed in explaining the observed spectra and transition probabilities. It is clear from Eq. (11) that a large  $\alpha_x$  amplifies the effects of mixing on the interband transition amplitudes.

The ratio of the reduced transition probabilities from a given state  $I_i$  to different final states within a band with angular momenta  $I_f$  and  $I_f'$  can be expressed as follows:

$$\frac{B(EL, I_i K_i \rightarrow I_f K_f)}{B(EL, I_i K_i \rightarrow I_f' K_f')} = F(\epsilon_x \alpha_x I_i I_f I_f' K_i K_f) \frac{|(I_i L K_i K | I_f K_f)|^2}{|(I_i L K_i K | I_f' K_f)|^2}, \quad (13)$$

where  $F$  may be regarded as a correction to the Alaga intensity rules. These ratios are plotted in Figs. 16(a), (b) for the de-excitation of two members of the beta and gamma bands, as functions of mixing parameters  $Z_\beta$  and  $Z_\gamma$  used previously in the literature.<sup>10</sup> The latter parameters are defined in the present notation as

$$Z_\beta = 2\epsilon_\beta \alpha_\beta; \quad Z_\gamma = (\sqrt{24})\epsilon_\gamma \alpha_\gamma. \quad (14)$$

The reduced transition-probability branching ratios measured in  $\text{Sm}^{152}$  are indicated in the figure as extended bold lines, the length specifying the error in measurement. These ratios differ somewhat from those based on preliminary data reported in a previous communication<sup>12</sup> due principally to a re-evaluation of the background for the 444-keV transition based on much more extensive and improved data. Table V lists the corresponding  $Z_\beta$  and  $Z_\gamma$  deduced from this analysis for each ratio measured. Two independent branching ratios are available for each band. It may be noted that some of the branching ratios are double-valued in  $Z$ ; however, in some cases one of these values can be excluded because of its unreasonably large magnitude. Here, both in the beta and gamma bands, the branching ratios  $B(E2, 2'2 \rightarrow 20)/B(E2, 2'2 \rightarrow 00)$  and  $B(E2, 2'0 \rightarrow 20)/B(E2, 2'0 \rightarrow 00)$  limit both  $Z_\gamma$  and  $Z_\beta$  to be negative, and there appears to be consistency between the values of  $Z$  obtained from the two ratios. It is unfortunate that because of interference from the population of the  $3^-$  state at 1045 keV, the branching ratio for the decay of the  $4^+$  state in the beta band could not be determined with confidence. Of course it is important to check the expected spin dependence of this band-mixing analysis. The poorly measured value for  $B(E2, 4'0 \rightarrow 40)/B(E2, 4'0 \rightarrow 20)$  of  $3.97 \pm 1.82$  is gratifyingly consistent with an average mixing parameter of  $Z_\beta = -0.066$  which predicts 3.25 for this ratio.

The parameter  $\epsilon_x$  enters directly into an evaluation of the corresponding energy perturbation of the ground-state rotational level structure. The displacement of a level of spin  $I$  is

$$E_I = -\epsilon_x^2 f_x^2(I) \hbar \omega_x, \quad (15)$$

where  $\hbar \omega_x$  represents the excitation energy of the band head of the beta or gamma bands. In order to extract  $\epsilon_x$  from the transition branching ratios in a model-independent way, without resorting to evaluation of the radial matrix elements from an assumed model for the vibrational wave functions,  $\alpha_x^2$  must be determined in an independent measurement, since only the product  $\alpha_x^2 \epsilon_x^2$  is determined from the transition probabilities. It has already been noted that the measurement of  $|Q(L; K_i K_f)|^2$  requires a knowledge of the mixing parameter  $Z_x$ , and that to minimize the error which may arise from the approximate way in which the band mixing has been considered in the multiple-Coulomb-excitation theory,  $B(E2, 00 \rightarrow 2'0)$  in the limit of zero mixing could best be obtained from the excitation of the  $0^+$  state. Here for  $Z_\beta = -0.066$ , the mixing correction is approximately 4% and 2% in the differential and total cross sections, respectively. The differential cross-section measurements were preferred over the total cross-section measurements for reasons already stated, and yielded a value for

$$|(0200|20)Q(2; 00)|^2 = (0.070 \pm 0.016)e^2 \times (10^{-48} \text{ cm}^4).$$

<sup>65</sup> M. A. Preston and D. Kiang, *Can. J. Phys.* **41**, 742 (1963).

<sup>66</sup> P. O. Lipas, *Nucl. Phys.* **40**, 629 (1963).

<sup>67</sup> R. K. Sheline, *Rev. Mod. Phys.* **32**, 1 (1960).

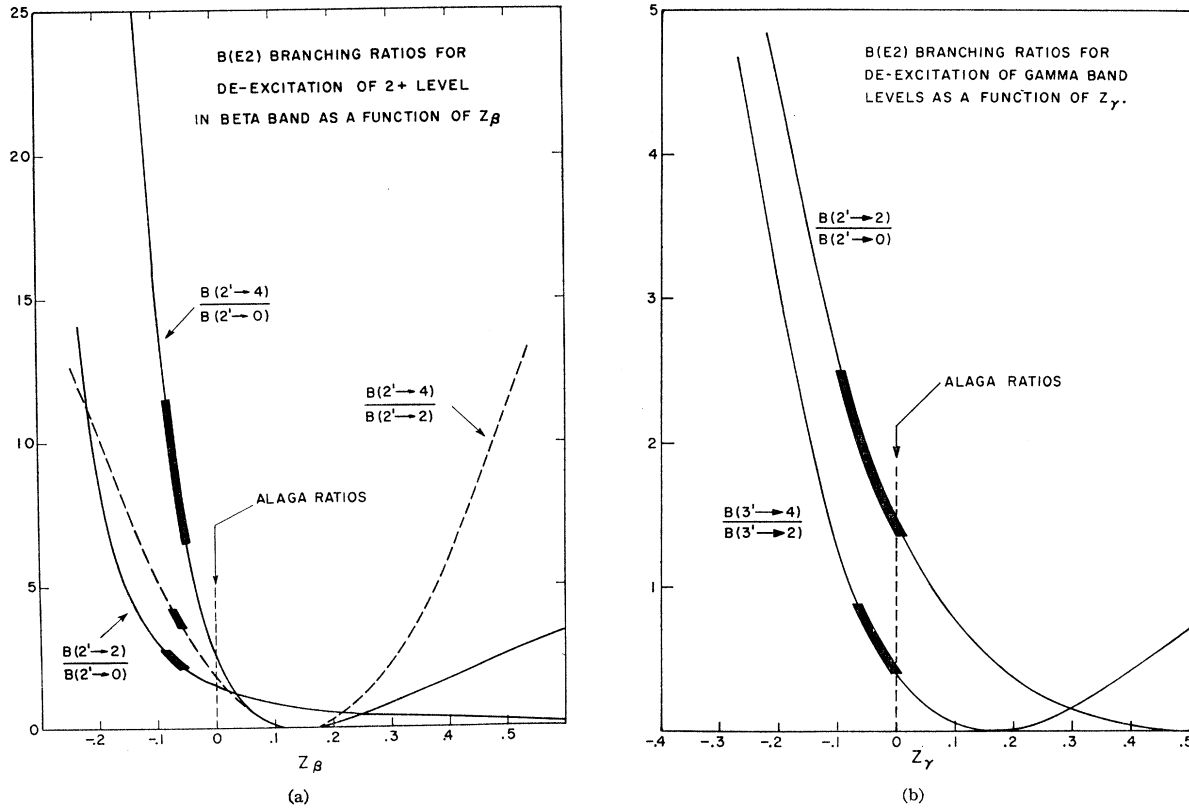


FIG. 16. (a). Ratios of reduced transition probabilities for the de-excitation of members of the beta band as a function of the mixing parameter  $Z_\beta$ . The bold lines indicate the range of measured values for  $\text{Sm}^{152}$ . (b). A similar plot for the gamma-band de-excitation reduced transition probability ratios.

The value for the latter quantity found from the measurement of the excitation of the  $2^+$  beta vibrational state was  $(0.052 \pm 0.007)e^2 \times (10^{-48} \text{ cm}^4)$ . The error on this value does not include uncertainties due to band-mixing effects, which may be large. The two values agree within the errors quoted but the latter is considered less reliable. Using the Elbek *et al.*,<sup>58</sup> measurement of  $B(E2, 00 \rightarrow 20) = (3.40 \pm 0.15)e^2 \times (10^{-48} \text{ cm}^4)$ , one has

$$\alpha_\beta^2 = 48.5 \pm 11.3.$$

The transition matrix element  $|(0202|22)Q(2;02)|^2$  for the gamma band was obtained from the total excitation probability to the band by adding together the cross section for the excitation of the  $2^+$ ,  $3^+$ , and  $4^+$  levels. Since the population of the  $4^+$  state in the gamma band is already down by more than an order of magnitude from the population of the  $2^+$  state, it is evident that the omission of higher spin states in this will only introduce a negligible error. Correcting for mixing as before, one obtains

$$|(0202|22)Q(2;02)|^2 = (0.119 \pm 0.024)e^2 \times (10^{-48} \text{ cm}^4),$$

which yields

$$\alpha_\gamma^2 = 28.6 \pm 5.5.$$

The error in estimating a mixing correction of 10% is not included.

It is of interest to point out that  $\alpha_\beta^2$  and  $\alpha_\gamma^2$  are thus much larger than predicted by the simple hydrodynamic model,<sup>65</sup> with axial symmetry, which yields for these two quantities:

$$\alpha_\beta^2 = 2 \frac{E(0^+, n_\gamma=0, n_\beta=1)}{E(2^+, n_\gamma=0, n_\beta=0)} = 11.26;$$

$$\alpha_\gamma^2 = \frac{E(2^+, n_\gamma=1, n_\beta=0)}{E(2^+, n_\gamma=0, n_\beta=0)} = 8.91.$$

In the treatment of nonadiabatic perturbations in axially symmetric nuclei discussed above, the large magnitude of  $\alpha_x^2$  appreciably reduces the effect of these perturbations on the rotational-energy-level spectrum, while it enhances these effects on the interband transition probabilities. It also may be noted that the transition moments from the ground state to the beta and gamma bands are, respectively, 2.9 and 5.1 single particle units, much smaller than usually found for vibrational states in the neighboring spherical nuclei. These values are typical for beta and gamma vibrations in the rare-earth deformed region ( $150 < A < 190$ ). The fundamental nature of these states is not yet clear;

TABLE VI. Values for the asymmetry parameter  $\gamma$  deduced from the experimental branching ratios of states in  $\text{Sm}^{152}$ .

Expt. transition ratios	$\gamma$ (deg)
$B(E2, 2' \rightarrow 0)/B(E2, 2' \rightarrow 2) = 0.535 \pm 0.183$	11.3
$B(E2, 3' \rightarrow 4)/B(E2, 3' \rightarrow 2) = 0.64 \pm 0.24$	7.5
$B(E2, 0 \rightarrow 2)/B(E2, 0 \rightarrow 2') = 31.2 \pm 6.5$	10.1

judging from the transition moments they appear to be only partially collective in character.

Turning now to an analysis of the measured transition probabilities in  $\text{Sm}^{152}$  in terms of the parameters of the asymmetric hydrodynamic rotor model, we find that for the adiabatic form of the model in which vibrations are excluded,<sup>14</sup> a somewhat inconsistent set of values for  $\gamma$  is obtained. Only included in these considerations are the de-excitations of members of the ground state and gamma bands in the Bohr-Mottelson designation, since beta vibrational states are excluded in the adiabatic asymmetric rotor model. The values for gamma resulting from consideration of the de-excitation branching ratios of the  $3^+$  and  $2'^+$  states and the excitation of the  $2^+$  and  $2'^+$  states are listed in Table VI. It is apparent that the average  $\gamma$  deduced from the transition probabilities is smaller than the value of  $\gamma = 13.2^\circ$  obtained from the energy ratio  $E(2'^+)/E(2^+)$  and very much smaller than the  $\gamma = 22^\circ$  calculated from  $E(4^+)/E(2^+)$ . This behavior has been observed previously<sup>17</sup> in the four even osmium isotopes,  $\text{Os}^{186}$  to  $\text{Os}^{192}$ , which span the transition region at the upper end of the rare earths.

In Table VII a comparison of the calculations by Davydov and Chaban is made with the measured transition branching ratios. These calculations incorporate the beta vibrations in the asymmetric hydrodynamic model in a manner outlined in the Introduction. Three parameters enter into the theory: the asymmetry parameter  $\gamma$ , the beta-vibrational band energy  $\hbar\omega_\beta$ , and the nonadiabaticity parameter  $\mu$ . For  $\mu < 0.25$ ,  $\mu$  may be approximated by  $E(2^+)/\hbar\omega_\beta$  where  $E(2^+)$  is the energy of the  $2^+$  state in the ground-state band. As one would expect, calculations show that  $\mu$  is most sensitive to the location of levels in the beta band

TABLE VII. A comparison of the experimental reduced transition probability branching ratios of states in  $\text{Sm}^{152}$  with the predictions of the Davydov-Chaban asymmetric rotor model with beta vibrations included. The theoretical reduced transition probability ratios were obtained from calculations by Davidson and Davidson.<sup>a</sup>

Transition ratio ( $M$ )	$M_{\text{expt}}$	$M_{\text{calc}}$ $\mu = 0.383$ $\gamma = 11.30^\circ$
$(0^+11 \rightarrow 2^+12)/(0^+11 \rightarrow 2^+11)$	$(1.32 \pm 0.30) \times 10^{-2}$	$3.5 \times 10^{-2}$
$(2^+12 \rightarrow 4^+11)/(2^+12 \rightarrow 2^+11)$	$3.79 \pm 0.67$	3.93
$(2^+12 \rightarrow 2^+11)/(2^+12 \rightarrow 0^+11)$	$2.36 \pm 0.70$	2.64
$(2^+21 \rightarrow 0^+11)/(2^+21 \rightarrow 2^+11)$	$0.535 \pm 0.183$	0.480 <sup>c</sup>

<sup>a</sup> J. P. Davidson and M. G. Davidson, Phys. Rev. **138**, B316 (1965).

and transition probabilities to this band, while being reasonably insensitive to the same quantities in the gamma band. The reverse is true for the parameter  $\gamma$ . Since we deal principally with energy and transition branching ratios, the over-all scale parameter  $\hbar\omega_\beta$  cancels out. The measured branching ratios are compared in Table VII with predictions for  $\mu = 0.383$  and  $\gamma = 11.3^\circ$  which were obtained from the two energy ratios  $E(2^+21)/E(2^+11)$  and  $E(0^+12)/E(2^+11)$ . The notation being used in  $E(I^\pi N n)$ , where  $I^\pi$  is the spin parity,  $N$  is the ordinal number of spin, and  $n$  is the ordinal number of  $\beta$  vibrations ( $n=1$  for ground-state band). Except for the ratio  $B(E2, 0^+11 \rightarrow 2^+11)/B(E2, 0^+11 \rightarrow 2^+12)$ , deduced from the Coulomb excitation measurement, the other three ratios show satisfactory agreement with the prediction for this  $\mu$  and  $\gamma$ . The Davydov-Chaban calculation requires a larger interband transition moment to the beta-vibrational states than that measured.

## VI. DISCUSSION

An examination of the energy-level structure in the four even samarium isotopes studied shows several distinguishing features. There is a rapid increase in the energies of the first  $2^+$  and  $4^+$  states with decreasing neutron number. In all four nuclei these states are collective in character, as can be inferred from their enhanced  $E(2)$  transition moments. The reduced transition probability ratio  $B(E2, 4^+ \rightarrow 2^+)/B(E2, 2^+ \rightarrow 0)$  is in agreement with the expected ratio for a rotational nucleus in  $\text{Sm}^{154}$  and  $\text{Sm}^{152}$  and for a pure vibrational nucleus in  $\text{Sm}^{150}$  and  $\text{Sm}^{148}$ . The abrupt change in character takes place at neutron number 88, and this is evident both from the energy-level structure and from the electromagnetic transition probabilities. It has already been noted by Emery *et al.*<sup>17</sup> that the transition region in Sm, Gd, and Nd nuclei is much more abrupt than that at the high-mass end of the deformed region in the even Os nuclei. As is also typical in the Os nuclei,<sup>17</sup> the second  $2^+$  state, which is usually referred to as a gamma vibration in rotational nuclei, decreases in energy with decrease in neutron number. More spectacularly, at the transition point between rotational and vibrational behavior, the  $K=0$  beta vibrational band drops in energy. In  $\text{Sm}^{152}$  the beta vibrational band head is located at 685 keV; for  $\text{Nd}^{150}$  and  $\text{Gd}^{154}$ , which occupy positions similar to  $\text{Sm}^{152}$  in their respective isotope sequences, the band head energies are, respectively at 687 keV<sup>31,68</sup> and 681 keV.<sup>45,31,68</sup> It is also characteristic of these beta bands that their moments of inertia are very similar to those of the ground-state bands ( $\sim 20$  keV) in contrast to the situation in the two negative parity octupole bands found in  $\text{Sm}^{152}$  and  $\text{Sm}^{154}$  where  $\hbar^2/2\mathcal{I} = 8.2$  keV and 10.0 keV, respectively. A possible source for this latter high effective moment of inertia is

<sup>68</sup> G. A. Burginyon and J. S. Greenberg, Bull. Am. Phys. Soc. **10**, 428 (1965).

a strong coupling with a nearby  $K=1$  band. No states which can be unambiguously attributed to the latter have thus far been reported in either of these nuclei.

Of special interest in the systematics of the excitation energies and transition strengths of the lowest  $3^-$  states in the four nuclei is the slow variation of both quantities with neutron number in a region where corresponding properties of the lowest lying quadrupole excitations exhibit a very rapid variation. It has been demonstrated that the energies of the lowest  $2^+$  states and the static quadrupole nuclear deformation are sensitive to the number of particles outside closed shells and to the residual interactions, whereas the  $3^-$  states are less sensitive to shell structure, although not entirely independent of it, as is clear from noting the variation of the energy of the  $3^-$  states with neutron number. A further rise in energy of these states occurs between neutron numbers 86 and 82 outside the region studied in this experiment, and the energy reaches approximately 2 MeV at neutron number 82. Hansen and Nathan<sup>37</sup> have reported an extensive survey of  $3^-$  levels over a large range of nuclei from  $A=106$  to 150 and have noted the qualitative decrease of the  $3^-$  excitation with  $A$ ; the general trend in excitation energy<sup>9,37</sup> is satisfactorily reproduced by taking 40% of the hydrodynamical-model predictions.

The attempt to account for some of the detailed properties of the level structure and transition moments in the four nuclei studied, in terms of the two principal phenomenological approaches referred to in the Introduction, has not been particularly successful. The information available, of course, is far from being complete enough for all the nuclei, but in the case of  $\text{Sm}^{152}$  there is presently sufficient information on hand to indicate significant incompatibilities with existing models.

$\text{Sm}^{154}$ .  $\text{Sm}^{154}$  is the most rotational nucleus of the four, and with the data available, provides almost no distinction between the models. The ground-state band excitations may be equally well described by a three-parameter expansion such as given in Eq. (1) for a perturbed symmetric rotor, or by the nonadiabatic, asymmetric hydrodynamic model. For the former the first three states are used to obtain  $A=13.82$  keV,  $B=-0.0268$  keV, and  $C=0.0016$  keV. The  $B$  and  $C$  terms are small, indicating small deviations from a simple rotor spectrum. With these parameters the  $8^+$  state is predicted at 916 keV which is to be compared with the measured value of  $905 \pm 9$  keV.

The adiabatic asymmetric model is unsuccessful if  $\gamma=9.5$ , as obtained from the energy ratio  $E(2^+)/E(2^+)$ , is used in the predictions. With this gamma, the  $4^+$ ,  $6^+$ , and  $8^+$  levels of the ground-state band are calculated to be at 273, 574, and 965 keV whereas the measured energies are, respectively, 267, 545, and 905 keV. These discrepancies are understandable since in the adiabatic model no allowance is made for the vibrational-rotational

interaction and for centrifugal stretching. If the Davydov-Chaban calculation, which includes the latter effects, is used on the basis of assumptions already mentioned, a very satisfactory fit is obtained with  $\mu=0.25$  and  $\gamma=8.9^\circ$ .

It has already been pointed out by several authors<sup>69</sup> that the asymmetric and symmetric models are essentially equivalent for small  $\gamma$  where the perturbing interactions mentioned above are small enough to justify treatment using perturbation techniques. For  $\mu$  as small as 0.25, the Davydov-Chaban energies may be expanded in a perturbation series, and, to first order, a correction term to the adiabatic asymmetric rotor is obtained which is equivalent to the  $B$  term in Eq. (1). The natural mixing of the wave functions of different quantum number  $K$ , in the asymmetric rotor model, is generated in the Bohr-Mottelson approach by the mixing mechanism between the ground state and gamma bands presented in Sec. IV. As  $\gamma$  approaches zero, the two calculations overlap in their predictions. The coefficient  $B$  contains, to lowest order, the interaction between both the  $K=0$  and  $K=2$  bands and the ground-state band.

$\text{Sm}^{152}$ . The situation is qualitatively different in  $\text{Sm}^{152}$ . A fit to the first two levels of the ground-state band, using only two terms of Eq. (1), yields  $A=21.15$  keV and  $B=-0.141$  keV. A three-parameter fit changes these coefficients considerably to  $A=21.39$  keV,  $B=-0.193$  keV and  $C=0.0020$  keV. It becomes immediately obvious that to adequately represent the energies of the ground-state band members in a power-series expansion in the angular momentum requires almost as many terms as there are experimental excitations. The series converges poorly with the zeroth-order wave functions as selected, and the usefulness of such an approach becomes questionable for a "soft rotor" such as  $\text{Sm}^{152}$ . It may be noted that similar large corrections to a simple-rotor prediction are obtained for the beta and gamma bands. For the former  $A=22.74$  keV,  $B=-0.289$  keV, and for the latter  $A=32.01$  keV,  $B=-0.399$  keV.

Ignoring for the moment the questions raised in the last paragraph, it was shown in Sec. V that the coefficient  $B$  in the angular-momentum expansion of the energy could be related to the measured branching ratios from the beta and gamma bands if it was assumed that the principal contribution to  $B$  originated in the rotational-vibrational interaction terms in a manner already specified. Then for the ground-state band,

$$B_\gamma = -\epsilon_\gamma^2 (\hbar\omega_\gamma) = -Z_\gamma^2 / 24\alpha_\gamma^2 (\hbar\omega_\gamma) \\ = -(0.075/\alpha_\gamma^2), \quad (16)$$

$$B_\beta = -\epsilon_\beta^2 (\hbar\omega_\beta) = -Z_\beta^2 / 4\alpha_\beta^2 (\hbar\omega_\beta) \\ = -(0.745/\alpha_\beta^2). \quad (17)$$

<sup>69</sup> Discussion by A. Bohr, *Proceedings of the International Conference on Nuclear Structure, Kingston, Ontario, 1960* (University of Toronto Press, Toronto, 1960), p. 807.



Using the measured values for the quantities on the right-hand side of Eqs. (11) and (12) yields  $B_\gamma = -0.003$  keV and  $B_\beta = -0.015$  keV. The sum is  $-0.018$  keV which is only 9% of the measured  $-0.193$  keV; thus band mixing, when treated in the manner outlined, obviously accounts for only a small fraction of the physics involved. This conclusion differs from some conjectures made in a previous publication,<sup>12</sup> which were based on earlier measurements and on the assumption that the values for  $\alpha_\beta^2$  and  $\alpha_\gamma^2$  could conceivably be as low as 10, which at that time was considered plausible when guided by the systematics of vibrational states. A direct measurement of these quantities was not available. However, as discussed in Sec. V, the measured reduced transition probabilities from the ground state to the beta and gamma bands are considerably reduced from the values naively expected for states of collective surface vibrations. This leads to values for  $\alpha_\beta^2$  and  $\alpha_\gamma^2$  considerably greater than 10 and therefore affects the final conclusion in a qualitative way. In addition, as mentioned above, a small discrepancy exists between the earlier and most recent data due to the re-evaluation of the intensity of the 444-keV transition from the beta band based on a more thorough examination of background effects in the newer and more exhaustive experiments.

Similar qualitative conclusions on the beta vibrational and ground-state band mixing have been reached by Yoshizawa *et al.*,<sup>65</sup> based on their gamma-particle coincidence measurements with  $O^{16}$  ions. The degree of mixing deduced from the latter measurements is somewhat larger than is quoted in the present work, although the two measurements agree within the quoted results and errors. However, it may be noted that in the gamma-particle coincidence data reported by Yoshizawa *et al.*, the 690-keV radiation from the  $2^+$  level in the beta-vibrational band is not resolved from transitions originating from the  $4^+$  state in the beta band and the  $3^-$  state in the octupole band. Particularly, a correction for the  $4^+$ -level de-excitation has not been made to the data in determining the intensity of the ( $2^+ \rightarrow 2^+$ ) transition used for the band-mixing calculations. As is pointed out by the above authors, this correction could alter the branching ratios significantly and hence the mixing coefficient. The gamma-gamma coincidence measurements performed in the present work and discussed in Sec. IV indicate that transitions from the  $4^+$  and  $3^-$  states comprise approximately 30% of the total composite gamma-ray peak at  $\sim 690$  keV in the singles gamma-ray spectrum. Furthermore, it is evident from Fig. 8 that the relative contribution from the  $4^+$  state to the total peak intensity is expected to be greatly enhanced in an experiment where the inelastically scattered particles are detected in coincidence in the backward direction, and therefore an appreciable correction is expected to the quoted result for the mixing coefficient obtained from the Yoshizawa *et al.* measurements. The correction is in a direction as to increase

$Z_\beta$  and increase the discrepancy between their value and ours. The discrepancy seems to be in the determination of the intensity of the 444-keV transition. The intensity of the 444-keV transition was evaluated in our experiment from the gamma-gamma coincidence data. In addition to the information the latter measurements supply on the transitions from the  $4^+$  and  $3^-$  states in the beta and octupole bands, respectively, we found that they lead to a more reliable determination of the 444-keV transition intensity than could be obtained from the gamma-particle coincidence data because of the larger error in evaluating the background in the gamma-particle spectrum resulting from the high intensity 563-keV transition and the transitions associated with the ground-state band.

It may be pointed out that the conclusion arrived at in the present analysis of band mixing agrees with the results derived from calculations of  $B$  from more fundamental microscopic considerations<sup>11</sup> where it is found that the rotational-vibrational interaction can only account for a very small fraction (1 to 10%) of the measured  $B$ . Additional contributions to  $B$  have been explored in a number of calculations<sup>11,70</sup> which indicate that the Coriolis-force antipairing effects may account for a significant fraction of the measured  $B$  and far exceed the contribution from the rotational-vibrational interaction.

Although the nonadiabatic hydrodynamic asymmetric rotor model produces a more satisfactory over-all fit to the total data than has been achieved with the mixing scheme just discussed, consideration of the details also points out some deficiencies. Except for one ratio, the measured branching ratios are reproduced, within experimental error, by  $\mu = 0.383$  and  $\gamma = 11.3^\circ$ . These values are obtained from the energy ratios  $E(2^+21)/E(2^+11)$  and  $E(0^+12)/E(2^+11)$  in the model notation. It is seen from the data presented in Table VII, however, that the values for  $\mu$  generally increase with increasing spin for the levels in the beta band, and decrease to fit the level energies in the ground-state band. The same effect may be evident for the ground-state band in  $Sm^{154}$ , although much reduced. The predicted location of the levels in the beta and ground-state bands are not very sensitive to the asymmetry parameter  $\gamma$ . The net effect of this behavior is to overestimate the excitation energies for the ground-state band members and underestimate the energies of members of the beta band when the values for  $\mu$  and  $\gamma$  are derived from the positions of the ( $0^+12$ ) state and the ( $2^+21$ ) state. The predicted energies for members of these two bands for  $\mu = 0.383$  and  $\gamma = 11.3^\circ$  are displayed in Table VIII. For the range of values for  $\gamma$  required to fit the ground-state and beta-band levels, physical values of  $\mu$  are excluded by the measured energies of the ( $3^+11$ ) and ( $4^+21$ ) states, i.e., a  $\mu < 0$  is required. For  $\mu = 0$  and

<sup>70</sup> T. Udagawa and R. K. Sheline, Phys. Rev. Letters 16, 325 (1966).



TABLE VIII. An analysis of the excitation energies in  $\text{Sm}^{152}$  in terms of the Davydov-Chaban asymmetric rotor model with beta vibrations included.

$I^\pi Nn$	$\gamma$	$\mu$	$[E(I^\pi Nn)/E(2^+11)]_{\text{expt}}$	$[E(I^\pi Nn)/E(2^+11)]_{\text{calc}}$ $\mu=0.383, \gamma=11.30^\circ$
4 <sup>+</sup> 11	11.50	0.374	3.009±0.002	2.98
6 <sup>+</sup> 11	11.60	0.365	5.70 ±0.06	5.55
0 <sup>+</sup> 12	11.30	0.383	5.62 ±0.01	
2 <sup>+</sup> 12	11.30	0.390	6.66 ±0.02	6.93
4 <sup>+</sup> 12	11.35	0.422	8.41 ±0.15	9.32
3 <sup>+</sup> 11	No solution	No solution	10.14 ±0.01	
4 <sup>+</sup> 21	No solution	No solution	11.35 ±0.02	

$\gamma=13.2^\circ$ , a very satisfactory agreement is obtained between the measured and calculated values for these latter states (Table IX). It is possible that the inclusion of the gamma degree of freedom into the Davydov-Chaban theory would resolve part of these discrepancies; the theory is certainly incomplete since it considers the nucleus rigid against gamma vibrations. Gamma vibrations have more recently been treated by Davydov,<sup>19</sup> but the numerical results are not presently available to make a comparison feasible. The  $\beta^2$  dependence assumed for the moment of inertia in the Davydov-Chaban calculation may be questioned as well as the exclusion of anharmonic terms in the potential which may be important for large deformations. Studies by Nilsson and Prior<sup>1</sup> and by Marshalek<sup>11</sup> indicated that the  $\beta^2$  dependence may be a poor approximation.

*Sm*<sup>148</sup> and *Sm*<sup>150</sup>. An application of the Davydov-Chaban model to *Sm*<sup>150</sup>, where there is sufficient data to make a marginal comparison, yields the following results. Using the position of the second 2<sup>+</sup> state and of the 0<sup>+</sup> state to determine  $\gamma=17^\circ$  and  $\mu=0.9$ , the energy of the 4<sup>+</sup> state is predicted to be 758 keV, as compared to the measured value of 773 keV. A 2<sup>+</sup> state is also predicted at an energy of 1170 keV which, with some imagination, may be identified tentatively with the known 2<sup>+</sup> state at 1193 keV. The measured branching ratios taken from this work and from studies by Groshev *et al.*,<sup>49</sup> on the other hand, do not compare nearly as well with predictions. No branching to the ground state from the 2<sup>+</sup> level at 1047 keV was observed in the present measurements. Groshev *et al.* reported  $B(E2, 2^+21 \rightarrow 0^+11)/B(E2, 2^+21 \rightarrow 2^+11)$  of 0.06. The value for this ratio predicted to correspond to  $\mu=0.9$  and  $\gamma=17^\circ$  is 0.22.

Both *Sm*<sup>148</sup> and *Sm*<sup>150</sup> exhibit some of the qualitative features predicted by a quadrupole surface phonon model where the surface energy is considered to be proportional to  $\beta^2$ . In *Sm*<sup>150</sup>, what would normally be considered as the second phonon triplet is grossly split, and the 2<sup>+</sup> state is situated somewhat higher in energy,  $E(2^+)/E(2^+)=3.14$ , than is customarily found in near spherical nuclei in the Pd-Cd region. One cannot, however, rule out the possibility of another 2<sup>+</sup> state close to the 4<sup>+</sup> and 0<sup>+</sup> which could be unresolved in this experiment.

An examination of the transition moments reveals a situation similar to that found in the Pd-Cd isotopes in that  $B(E2, 2^+ \rightarrow 4^+)/B(E2, 0^+ \rightarrow 2^+)$  is roughly in accord with the predictions of the pure phonon model, while a similar ratio involving the second 2<sup>+</sup> state, assuming correct identifications, falls short of the model predictions. The second 0<sup>+</sup> state in *Sm*<sup>150</sup> appears to be collective as judged from the measured transition moment to that state. The addition of anharmonic terms in the potential and the introduction of coupling of vibrations to particle motion may account for some of the splitting of the triplet levels; however, no definitive results have yet been found from such studies.

It is evident from the above discussion that although the phenomenological models, with the modifications considered above, can reproduce some of the general features of the observed excitation spectra and transition matrix elements in the even samarium isotopes, they are unable to do so in detail. The results from *Sm*<sup>152</sup> indicate that for very soft rotors the axially symmetric model with a first-order perturbation treatment of the rotational-vibrational interaction is not adequate to explain the structure of the low-lying states. Because of its poor convergence, the expansion of the excitation energy of rotational-band members in a power series in the angular momentum does not constitute a fruitful procedure for such nuclei. The more exact account of centrifugal stretching evolved by Davydov and Chaban presently produces a better overall fit to the data. It is significant that reasonably good agreement between the Davydov-Chaban model and experiment is obtained for the  $B(E2)$  values for transitions from the beta band and for the ground-state and beta-band energies. How-

TABLE IX. A comparison of the predictions of the simple asymmetric rotor model with  $\gamma=13.2^\circ$  with excitation energies in *Sm*<sup>152</sup>. The value for  $\gamma$  was deduced from the ratio  $E(2^+)/E(2^+)$ .

$I^\pi$	$E(I)_{\text{calc}}$ (keV) $\mu=0, \gamma=13.2^\circ$	$E(I)_{\text{expt}}$ (keV)
4 <sup>+</sup>	402	367
6 <sup>+</sup>	830	707
3 <sup>+</sup>	1216	1236
4 <sup>+</sup>	1386	1382

ever the remaining discrepancies indicate that this model requires further development.

### ACKNOWLEDGMENTS

We wish to thank Professor E. R. Beringer and the staff of the Yale HILAC for their assistance during the course of this experiment. The Yale authors would wish to express their appreciation to Dr. C. D. Moak and

Dr. P. H. Stelson for their help and hospitality during their stay at the High Voltage Laboratory at ORNL. We are indebted to Professor E. R. Beringer and to Dr. Joseph Weneser for stimulating discussion concerning this work. The participation of E. V. Bishop and G. A. Burginyon in apparatus development and some phases of data accumulation is gratefully acknowledged.

## Alteration of the Decay Constant of $\text{Te}^{125m}$ by Chemical Means\*

A. C. MALLIARIS AND KENNETH T. BAINBRIDGE

*Lyman Laboratory of Physics, Harvard University, Cambridge, Massachusetts*

(Received 4 April 1966)

The total rate of a nuclear transition which proceeds partially by internal conversion may be expected to change when alterations are produced in the states of the electrons concerned. Such alterations may be produced, for instance, by chemical means. Differences in the decay constant of the highly converted isomeric transitions of  $\text{Te}^{125m}$  have been measured using Te,  $\text{TeO}_2$ , and  $\text{Ag}_2\text{Te}$  (synthetic hessite). The results are:  $\lambda(\text{Te}) - \lambda(\text{Ag}_2\text{Te}) = (2.59 \pm 0.18) \times 10^{-4} \lambda(\text{Te})$ ;  $\lambda(\text{TeO}_2) - \lambda(\text{Ag}_2\text{Te}) = (2.23 \pm 0.18) \times 10^{-4} \lambda(\text{Te})$ ;  $\lambda(\text{Te}) - \lambda(\text{TeO}_2) = (0.36 \pm 0.17) \times 10^{-4} \lambda(\text{Te})$ . The errors are standard deviations arising mainly from the statistical fluctuations of the number of ionizing events which contributed to a measurement by the double-ionization-chamber balance method. The ionization currents were produced by the  $K$  x rays following the internal conversion process in the sources. Corrections were made for the effect of an initial 0.05% contamination of  $\text{Te}^{125m}$ . Sources of errors are considered in detail.

### I. INTRODUCTION

THE decay constant of an isomer may be changed by external means if the outer electrons participate appreciably in the transition.<sup>1</sup> For example, a change of the chemical environment of the atoms concerned may cause a change of the electron density in the appropriate domain, thus speeding or slowing the nuclear transition.<sup>2</sup> Alterations in the decay rate have been produced also by applied high pressure,<sup>3</sup> as well as by bringing the element concerned into its superconducting state.<sup>4</sup>

This paper presents detailed results showing that the decay rate of the highly converted isomeric transition in  $\text{Te}^{125m}$  depends upon the chemical state of combination of the tellurium.<sup>5</sup> The decay constants were compared for  $\text{Te}^{125m}$  in Te (elemental),  $\text{TeO}_2$ , and  $\text{Ag}_2\text{Te}$  (synthetic hessite).

The decay scheme of  $\text{Te}^{125m}$  is given in Fig. 1.<sup>6</sup> The half-life is approximately 58 days. Since, as shown in Fig. 1, the outer electrons participate in the internal conversion process and there is no crossover transition, it appeared that the transition rate might be altered by chemical means. Another factor in the selection of  $\text{Te}^{125m}$  for these experiments was that tellurium under pressure undergoes a polymorphic transition and changes from a poor to a metallic conductor.<sup>7</sup> If  $\text{Te}^{125m}$  responded to the chemical influence, such a result would encourage extension of the experiments to later study of the possible effects of the interesting changes in lattice structure and electrical conductivity induced by pressure.

The decay rates of the different sources were compared by the differential ionization chamber method described in Ref. 2, but the steel chambers were spherical

\* Research supported in part by the Navy Department (Office of Naval Research) under ONR Contract Nonr-1866(19).

<sup>1</sup> R. Daudel, *Rev. Sci.* **85**, 162 (1947); and M. Goldhaber (unpublished lectures).

<sup>2</sup> K. T. Bainbridge, M. Goldhaber, and E. Wilson, *Phys. Rev.* **84**, 1260 (1951); **90**, 430 (1953); J. A. Cooper, J. M. Hollander, and J. O. Rasmussen, *Phys. Rev. Letters* **15**, 680 (1965); S. Shimizu and H. Mazaki, *Phys. Letters* **17**, 275 (1965).

<sup>3</sup> K. T. Bainbridge, *Chem. Eng. News* **30**, 654 (1952); R. A. Porter and W. G. McMillan, *Phys. Rev.* **117**, 795 (1960).

<sup>4</sup> D. H. Byers and R. Stump, *Phys. Rev.* **112**, 77 (1958).

<sup>5</sup> M. Goldhaber (private communication) mentioned  $\text{Te}^{125m}$  as an isomer which might show an effect.

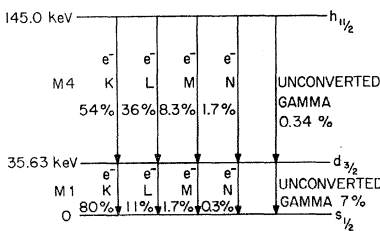


FIG. 1. The decay scheme of  $\text{Te}^{125m}$ .

<sup>6</sup> R. Narcisi, thesis, Harvard University, 1959 (unpublished).

<sup>7</sup> P. W. Bridgman, *Proc. Am. Acad. Arts Sci.* **81**, 167 (1952).